Pionic atom unveils hidden structure of QCD vacuum

—Deduction of chiral condensate at nuclear density—

RIKEN Nishina Center

Kenta Itahashi

Pionic atom unveils hidden structure of QCD vacuum

Takahiro Nishi[1], Kenta Itahashi[1,*] DeukSoon Ahn[1,2], Georg P.A. Berg[3], Masanori Dozono[1], Daijiro Etoh[4], Hiroyuki Fujioka[5], Naoki Fukuda[1], Nobuhisa Fukunishi[1], Hans Geissel[6], Emma Haettner[6], Tadashi Hashimoto[1], Ryugo S. Hayano[7], Satoru Hirenzaki[8], Hiroshi Horii[7], Natsumi Ikeno[9], Naoto Inabe[1], Masahiko Iwasaki[1], Daisuke Kameda[1], Keichi Kisamori[10], Yu Kiyokawa[10], Toshiyuki Kubo[1], Kensuke Kusaka[1], Masafumi Matsushita[10], Shin'ichiro Michimasa[10], Go Mishima[7], Hiroyuki Miya[1], Daichi Murai[1], Hideko Nagahiro[8], Megumi Niikura[7], Naoko Nose-Togawa[11], Shinsuke Ota[10], Naruhiko Sakamoto[1], Kimiko Sekiguchi[4], Yuta Shiokawa[4], Hiroshi Suzuki[1], Ken Suzuki[12], Motonobu Takaki[10], Hiroyuki Takeda[1], Yoshiki K. Tanaka[1], Tomohiro Uesaka[1], Yasumori Wada[4], Atomu Watanabe[4], Yuni N. Watanabe[7], Helmut Weick[6], Hiroki Yamakami[5], Yoshiyuki Yanagisawa[1], and Koichi Yoshida[1]

https://doi.org/10.48550/arXiv.2204.05568

Material properties of vacuum

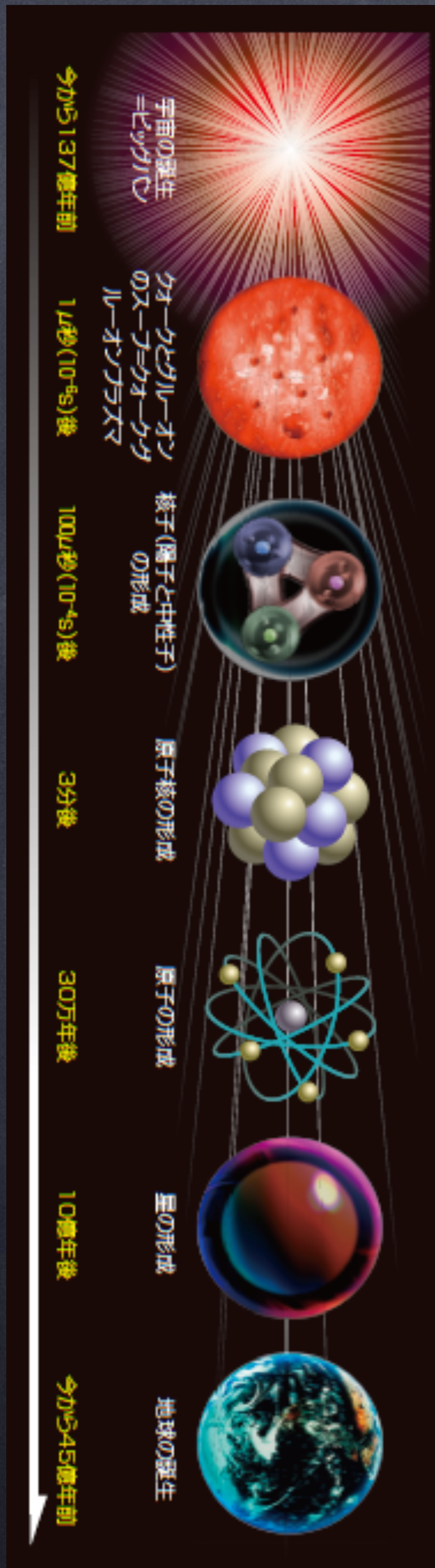

Properties of QCD vacuum
depend on temperature and matter-density

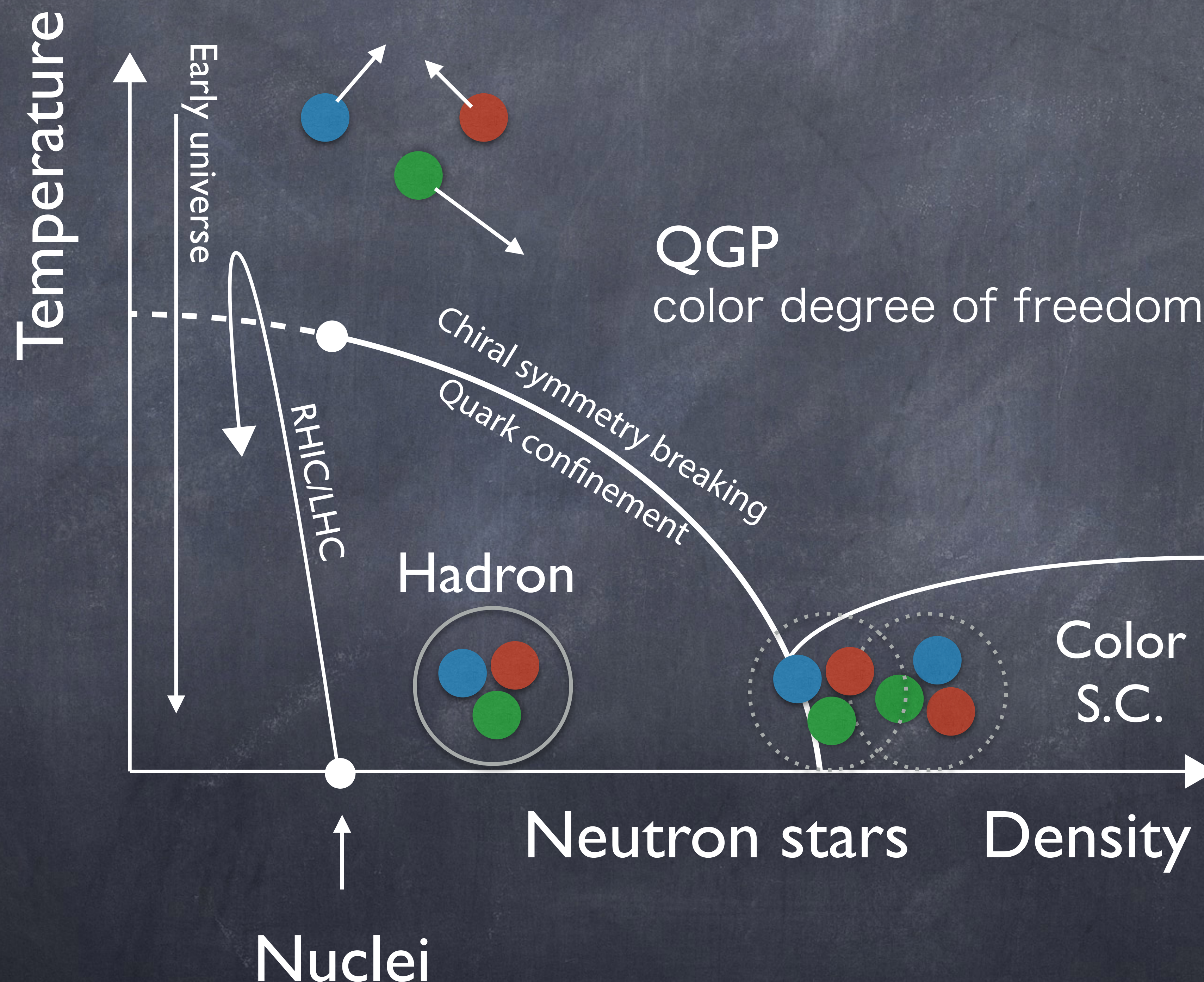

QCD phase and chemical freezeout points

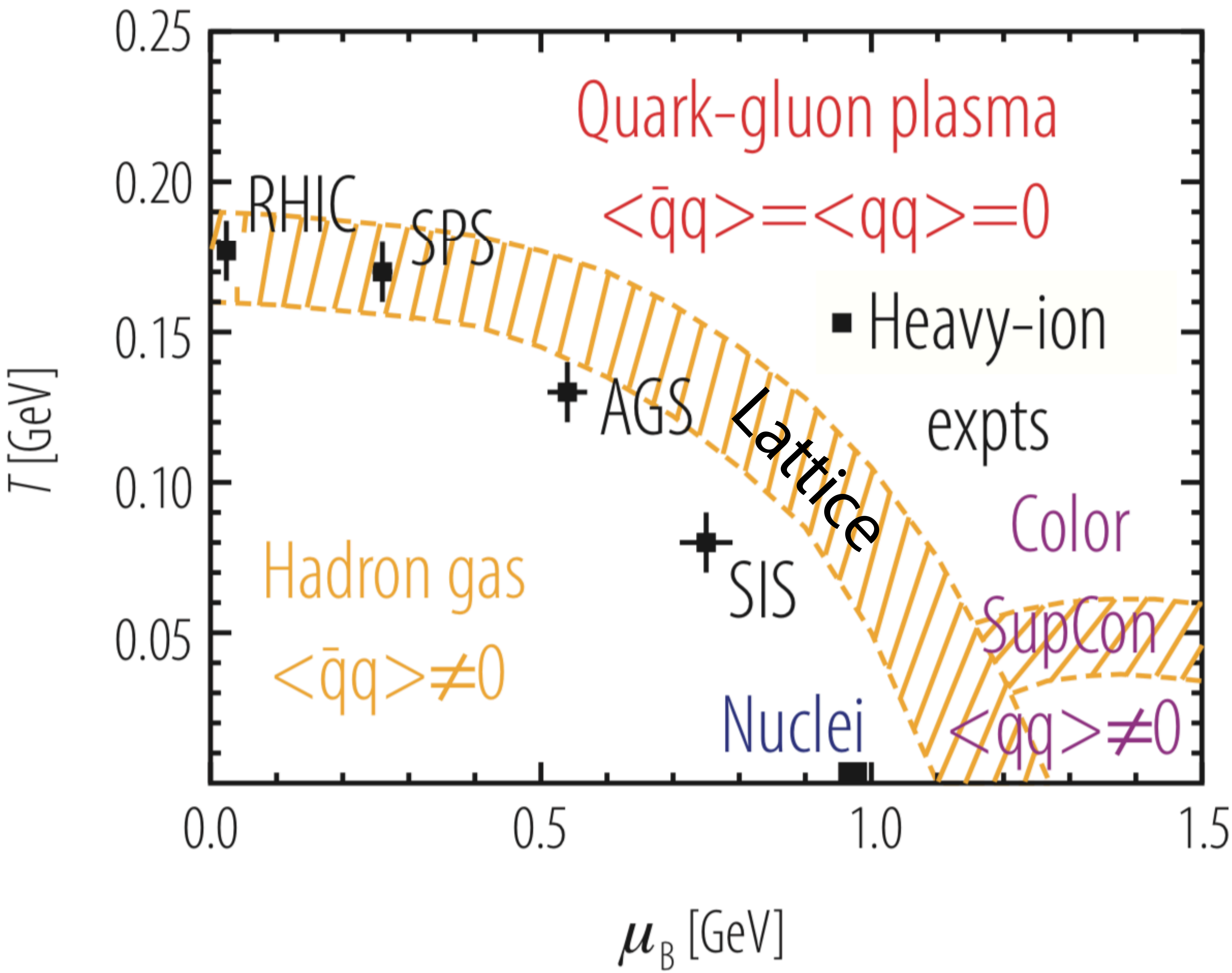

Rapp, Wambach, Hees, SpringerMaterials 23, 1 (2010)

Chiral transition & Quark confinement

Correlation between Confinement and CSB is suggested by
Simultaneous Phase Transition of
Deconfinement and Chiral Restoration.

Lattice QCD results at finite temperature F. Karsch, Lect. Notes Phys. (2002)

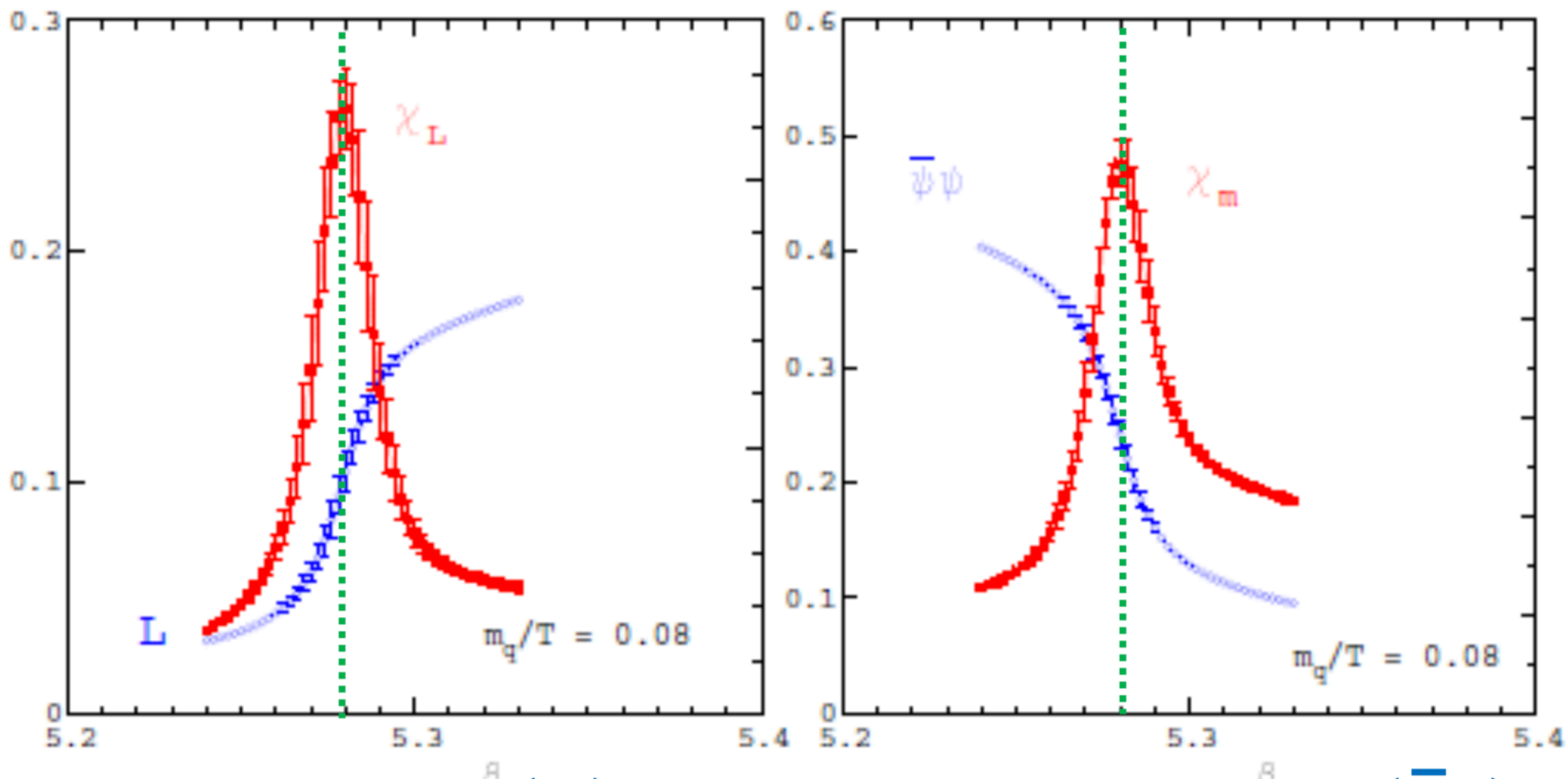

Polyakov Loop **<P>** Chiral Condensate **<$\bar{q}q$>**

Color Confinement Chiral Symmetry Breaking

Fig. 2. Deconfinement and chiral symmetry restoration in 2-flavour QCD: Shown is $\langle L \rangle$ (left), which is the order parameter for deconfinement in the pure gauge limit ($m_q \to \infty$), and $\langle \bar{\psi}\psi \rangle$ (right), which is the order parameter for chiral symmetry breaking in the chiral limit ($m_q \to 0$). Also shown are the corresponding susceptibilities as a function of the coupling $\beta = 6/g^2$.

H. Suganuma, JPS symposium (2010)

Chiral transition & Quark confinement

Correlation between Confinement and CSB is suggested by
Simultaneous Phase Transition of
Deconfinement and Chiral Restoration.

Lattice QCD results at finite temperature F. Karsch, Lect. Notes Phys. (2002)

Confinement と Chiral Symmetry Breaking の相関

有限温度や有限体積効果でのQCD相転移の様相などから、
両者には密接な対応関係があるのは明らか
～Deconfinement と Chiral Symmetry Restoration の一致

ただし、両者の関係はあまり良く分かっていないのが現状

Polyakov Loop ＜**P**＞ Chiral Condensate ＜$\bar{\mathbf{q}}\mathbf{q}$＞

Color Confinement Chiral Symmetry Breaking

Fig. 2. Deconfinement and chiral symmetry restoration in 2-flavour QCD: Shown is $\langle L \rangle$ (left), which is the order parameter for deconfinement in the pure gauge limit ($m_q \to \infty$), and $\langle \bar{\psi}\psi \rangle$ (right), which is the order parameter for chiral symmetry breaking in the chiral limit ($m_q \to 0$). Also shown are the corresponding susceptibilities as a function of the coupling $\beta = 6/g^2$.

H. Suganuma, JPS symposium (2010)

Lattice QCD calculated T dependence of chiral condensate

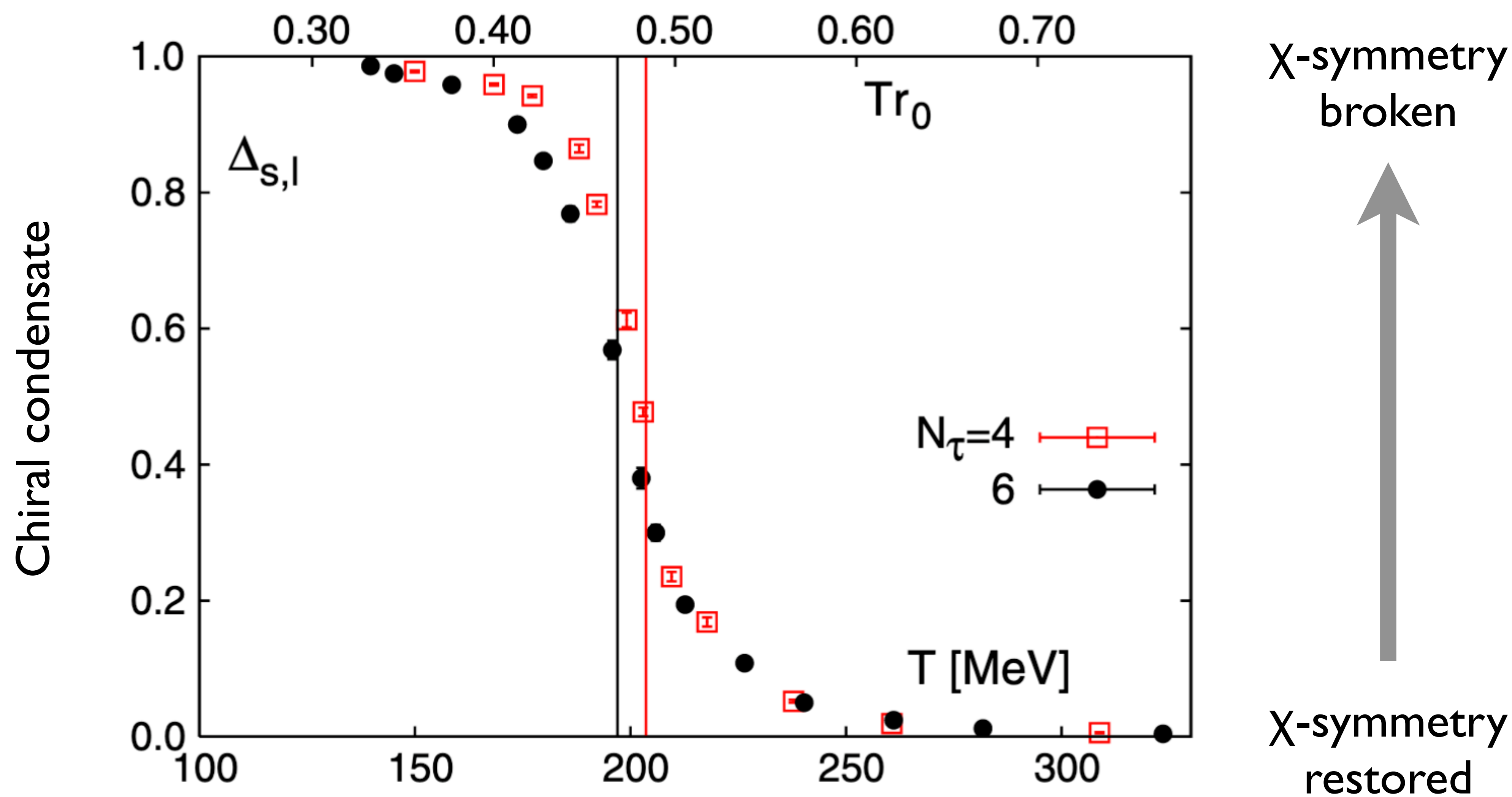

Temperature dependence of the chiral condensate from lattice QCD with 2 + 1 quark flavours and almost physical quark masses

M. Cheng et al., Phys. Rev. D77(2008), 014511.

Lattice QCD calculated T dependence of chiral condensate

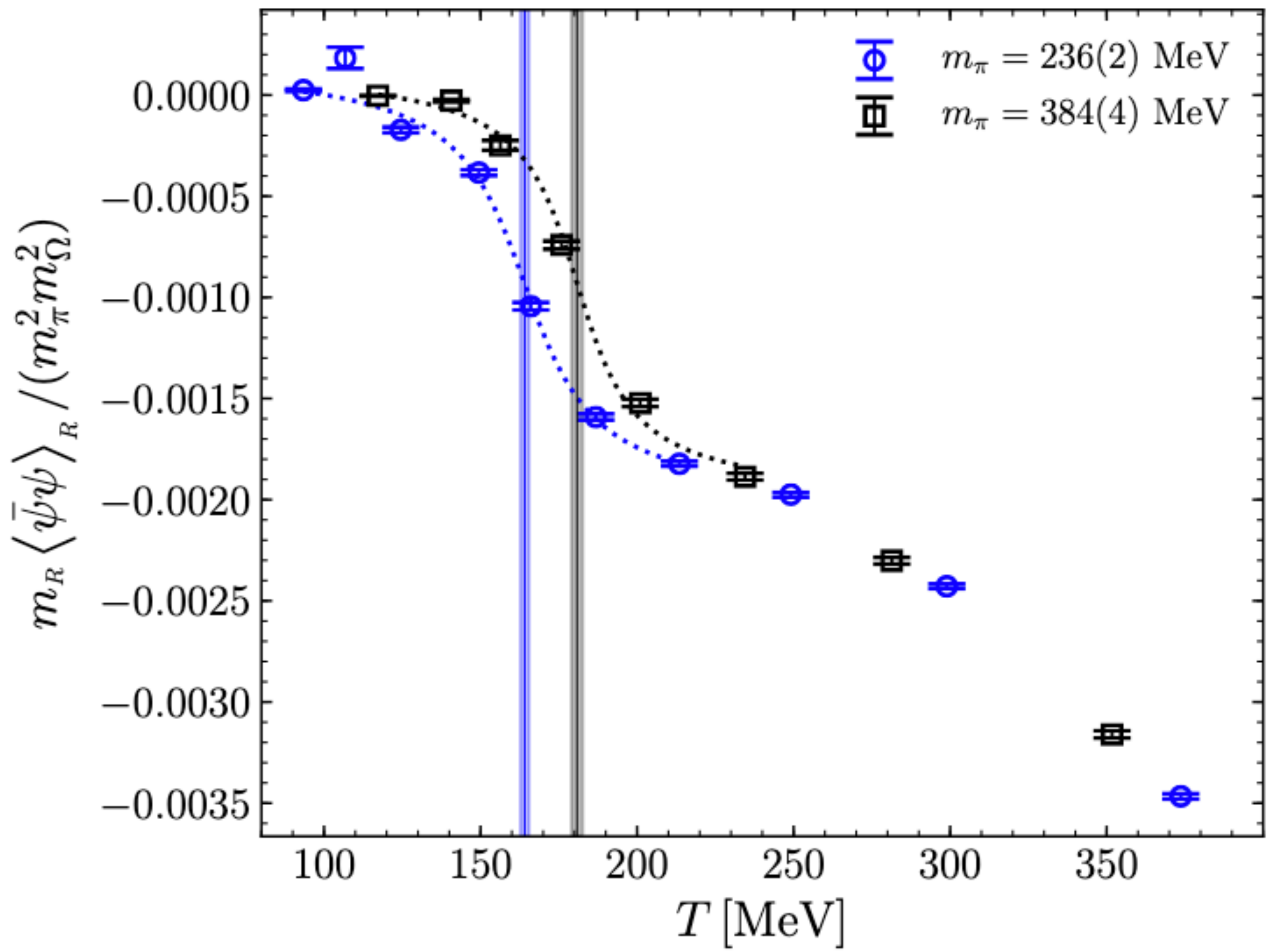

χ-symmetry broken

χ-symmetry restored

Remark: sign problem makes it difficult for lattice to approach non-zero ρ region

Jon-Ivar Skullerud
PRD105(2022)034504

Chiral condensate, order parameter of chiral symmetry

One of order parameters of
χ-symmetry breaking:

Chiral condensate

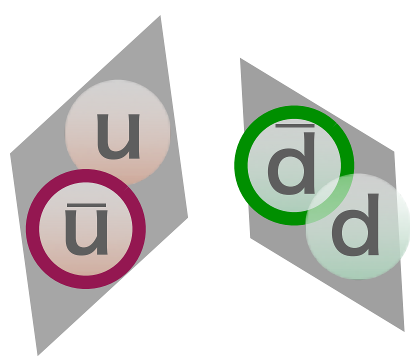

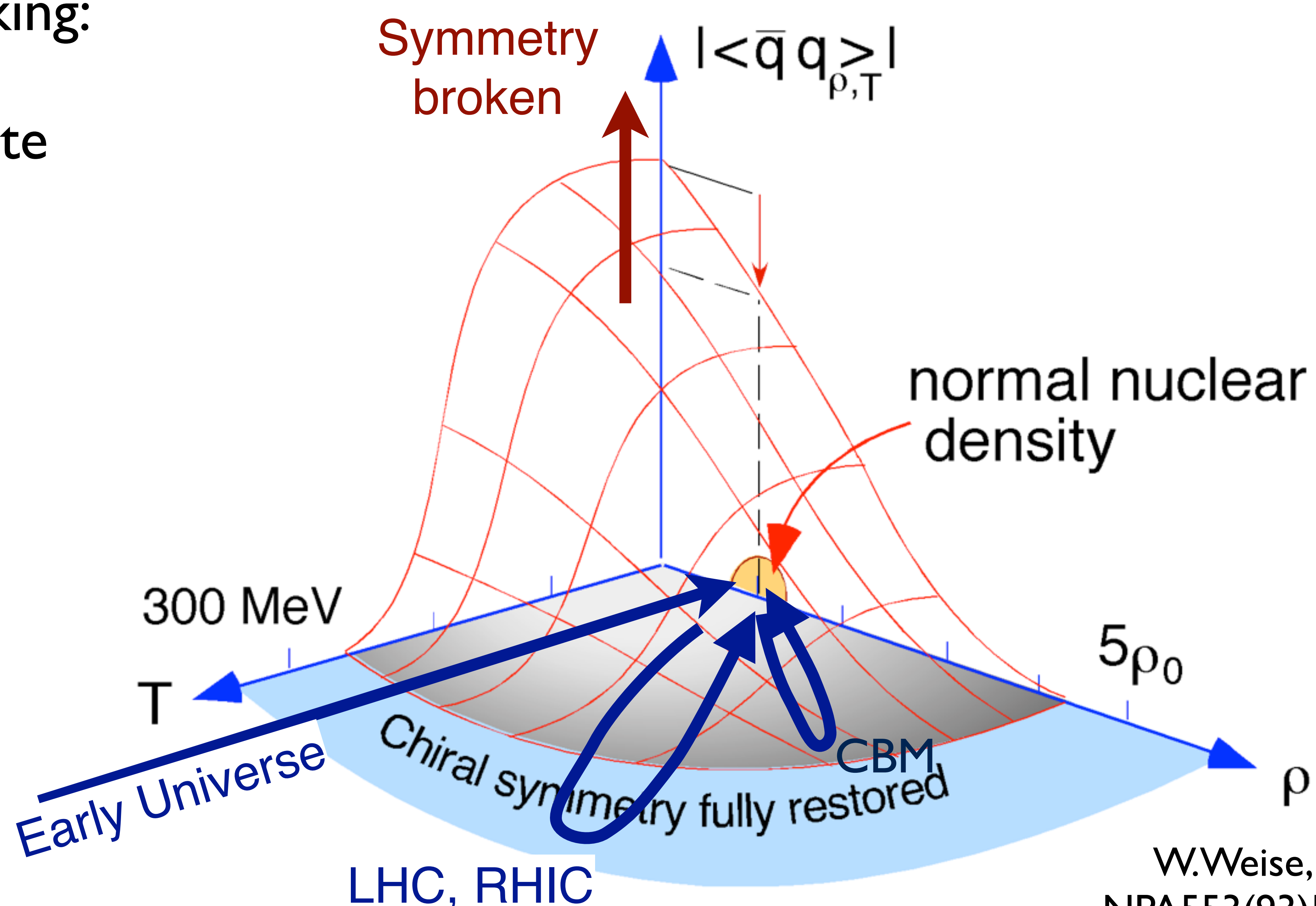

W.Weise, NPA553(93)59.

Remark: sign problem makes it difficult for lattice to approach non-zero ρ region

Analysis of material properties of QCD vacuum

ρ dependence of chiral condensate

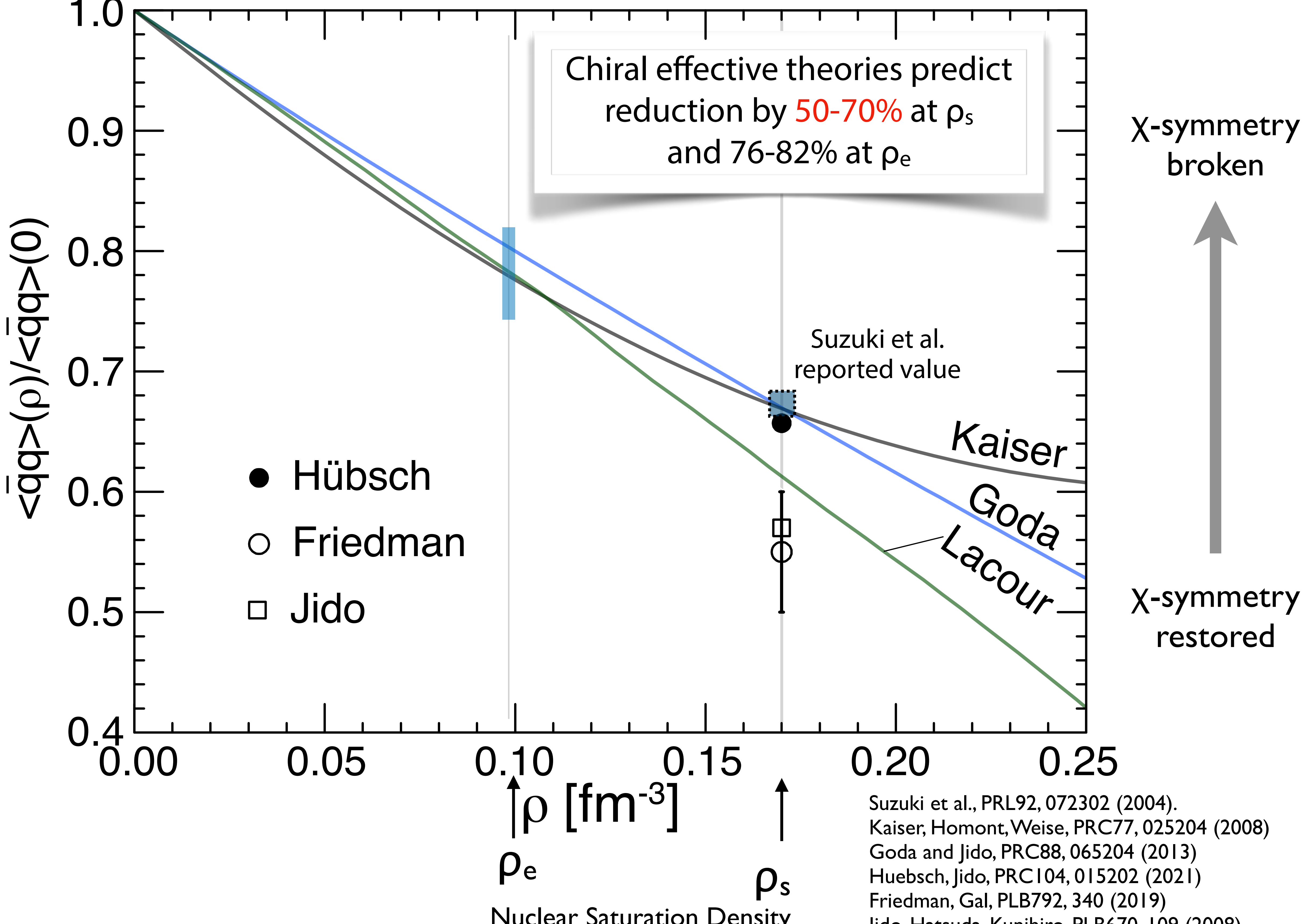

Suzuki et al., PRL92, 072302 (2004).
Kaiser, Homont, Weise, PRC77, 025204 (2008)
Goda and Jido, PRC88, 065204 (2013)
Huebsch, Jido, PRC104, 015202 (2021)
Friedman, Gal, PLB792, 340 (2019)
Jido, Hatsuda, Kunihiro, PLB670, 109 (2008)
Lacour, Oller, Meissner, J. Phys. G. 37, 125002 (2010)

Meson masses and QCD medium effect

Vector meson mass modification

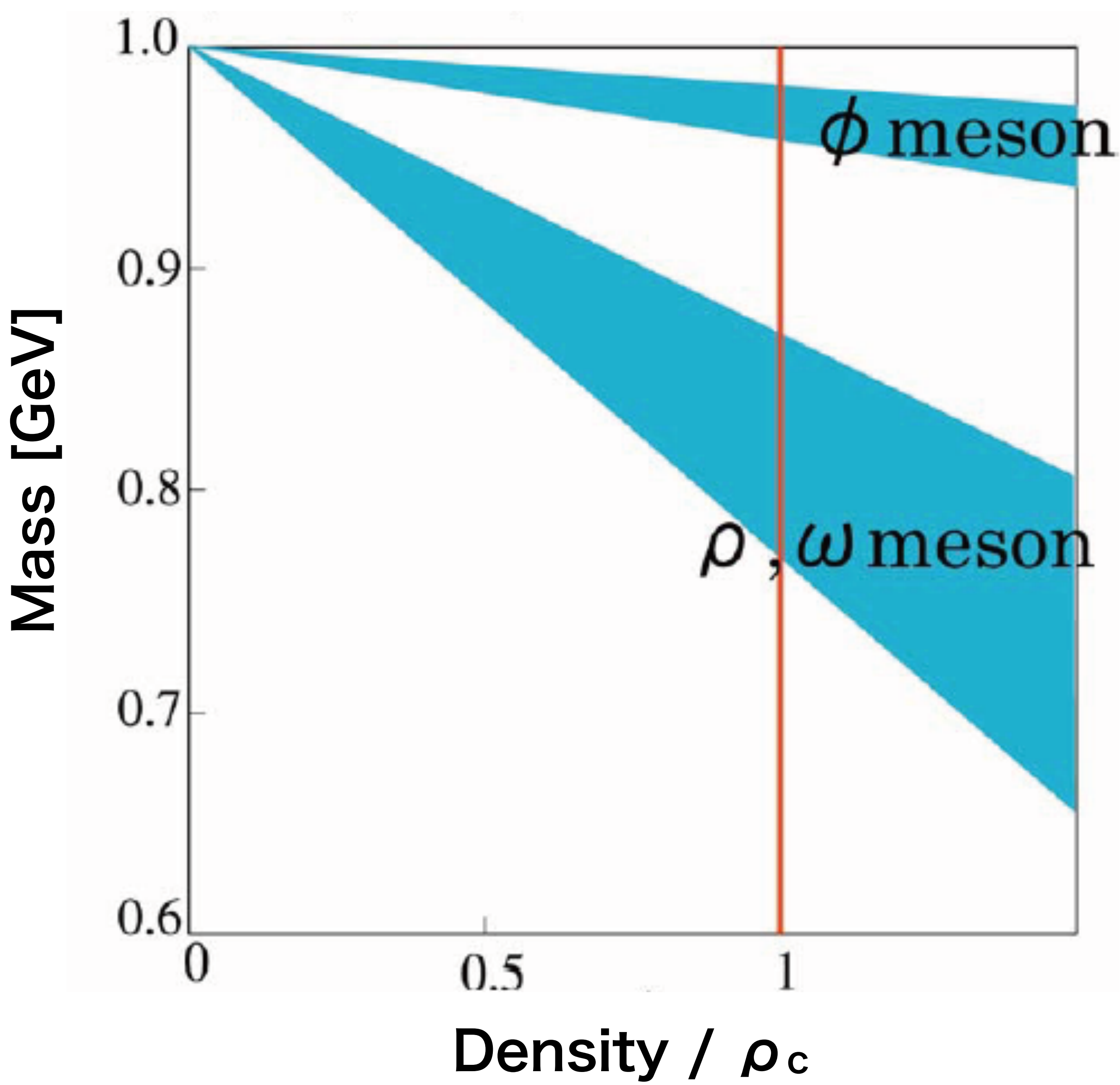

ϕ(1020) $I^G(J^{PC}) = 0^-(1^{--})$

Mass $m = 1019.455 \pm 0.020$ MeV (S = 1.1)
Full width $\Gamma = 4.26 \pm 0.04$ MeV (S = 1.4)

ϕ(1020) DECAY MODES	Fraction (Γ_i/Γ)	Scale factor/ Confidence level	p (MeV/c)
K^+K^-	(48.9 ± 0.5) %	S=1.1	127
$K_L^0 K_S^0$	(34.2 ± 0.4) %	S=1.1	110
$\ell^+\ell^-$	—		510
e^+e^-	$(2.954 \pm 0.030) \times 10^{-4}$	S=1.1	510
$\mu^+\mu^-$	$(2.87 \pm 0.19) \times 10^{-4}$		499

ρ(770) [h] $I^G(J^{PC}) = 1^+(1^{--})$

Mass $m = 775.49 \pm 0.34$ MeV
Full width $\Gamma = 149.1 \pm 0.8$ MeV
$\Gamma_{ee} = 7.04 \pm 0.06$ keV

ω(782) $I^G(J^{PC}) = 0^-(1^{--})$

Mass $m = 782.65 \pm 0.12$ MeV (S = 1.9)
Full width $\Gamma = 8.49 \pm 0.08$ MeV
$\Gamma_{ee} = 0.60 \pm 0.02$ keV

T.Hatsuda, S.H.Lee, Phys. Rev. ***C46*** *(1992) R34*

Brown,Rho(1991), Hatsuda,Lee(1992)
Klingle,Keiser,Weise(1997),etc.

Masses of Pseudo-Scalar Mesons

with various symmetry breaking patterns

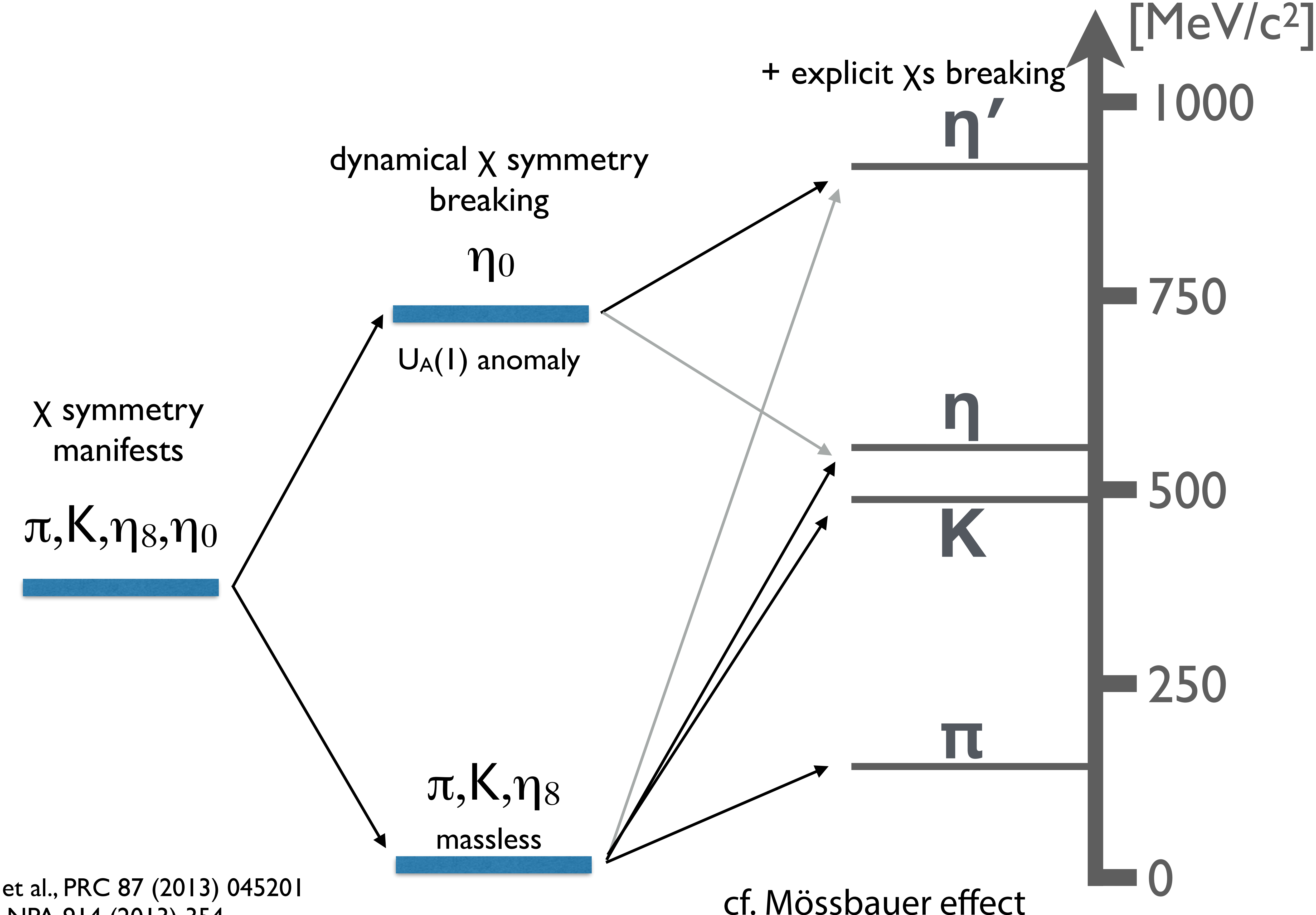

Nagahiro et al., PRC 87 (2013) 045201
Jido et al., NPA 914 (2013) 354

PS in high density medium

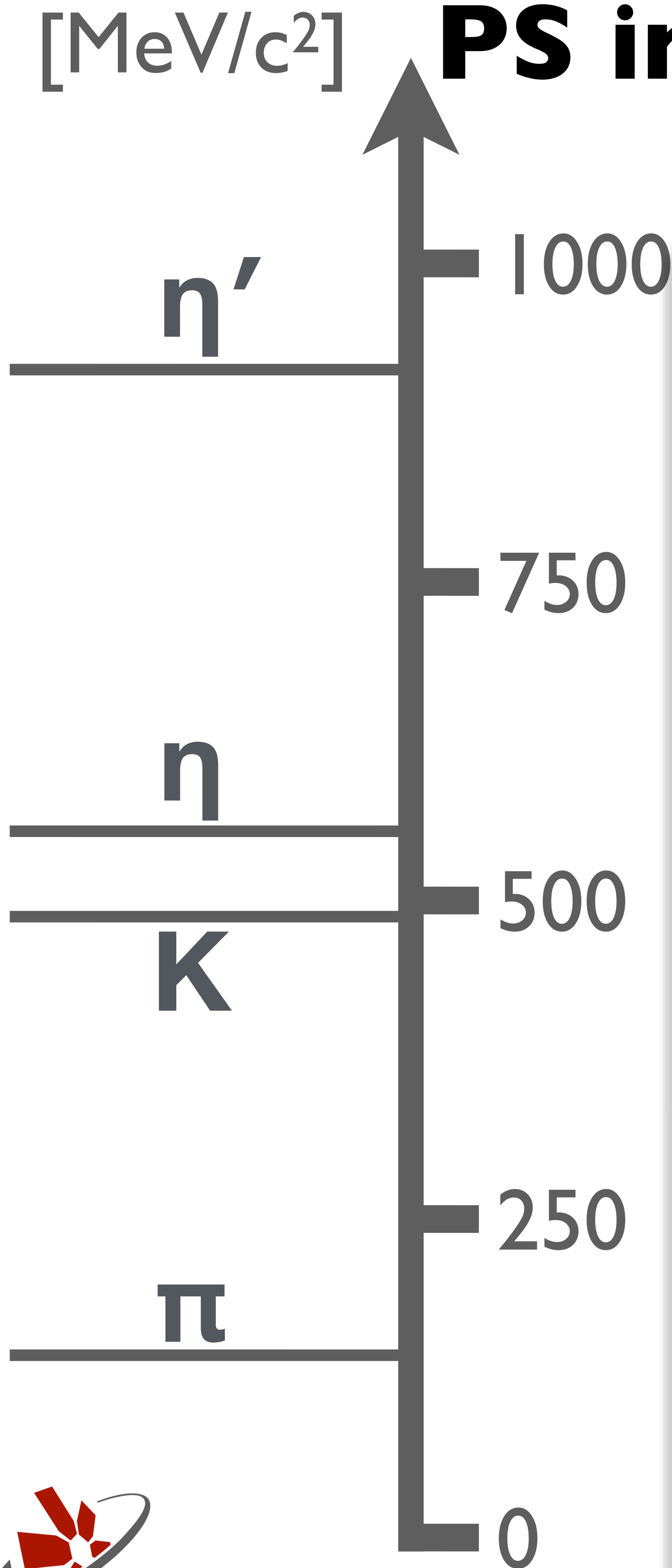

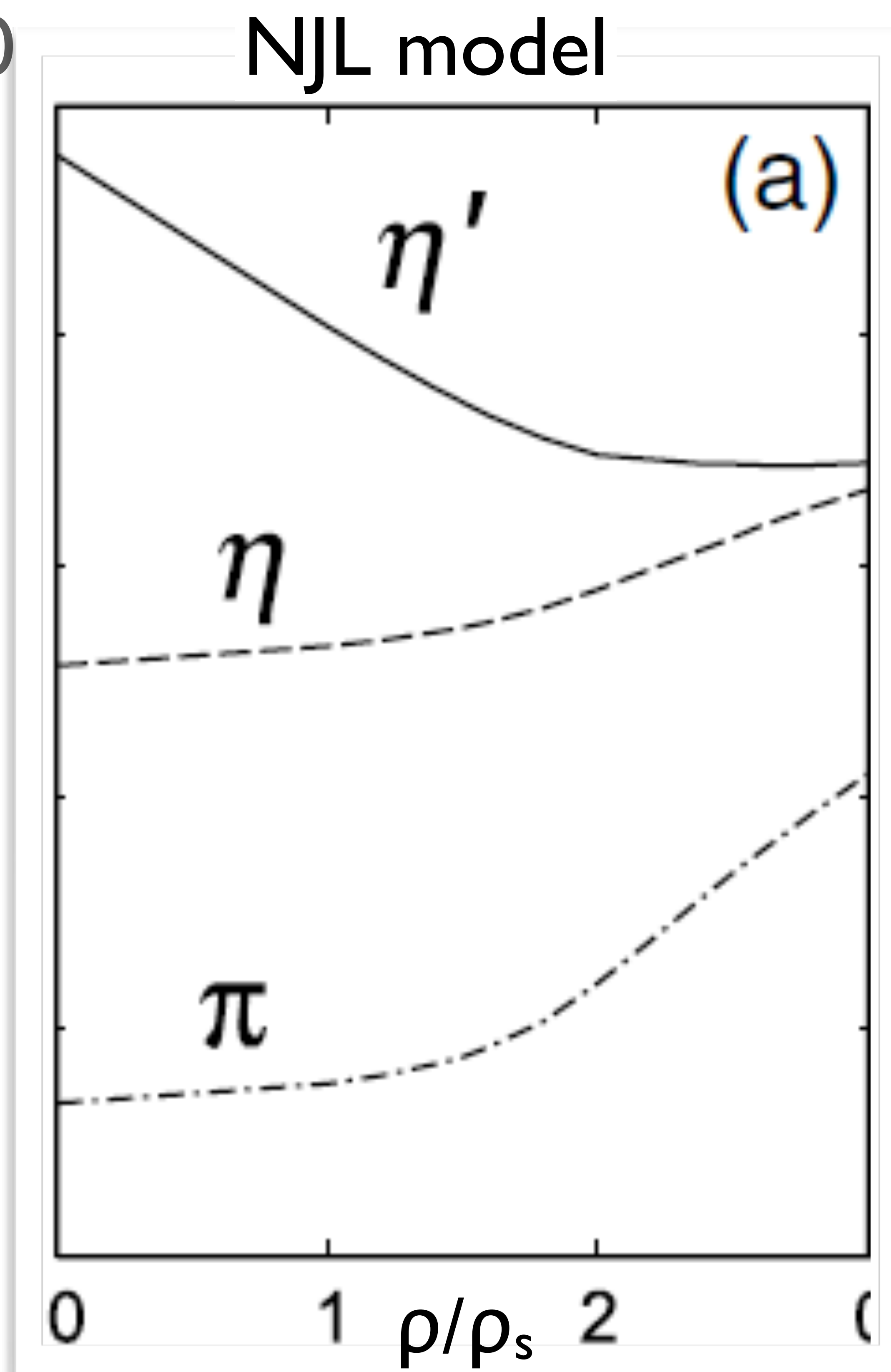

REMARK

⊿m between
η-η′, (σ, π)
(ρ, a1) are important

Nagahiro *et al*, PRC 74, 045203 (2006)

RIKEN NiSHiNA CENTER

Pionic atoms

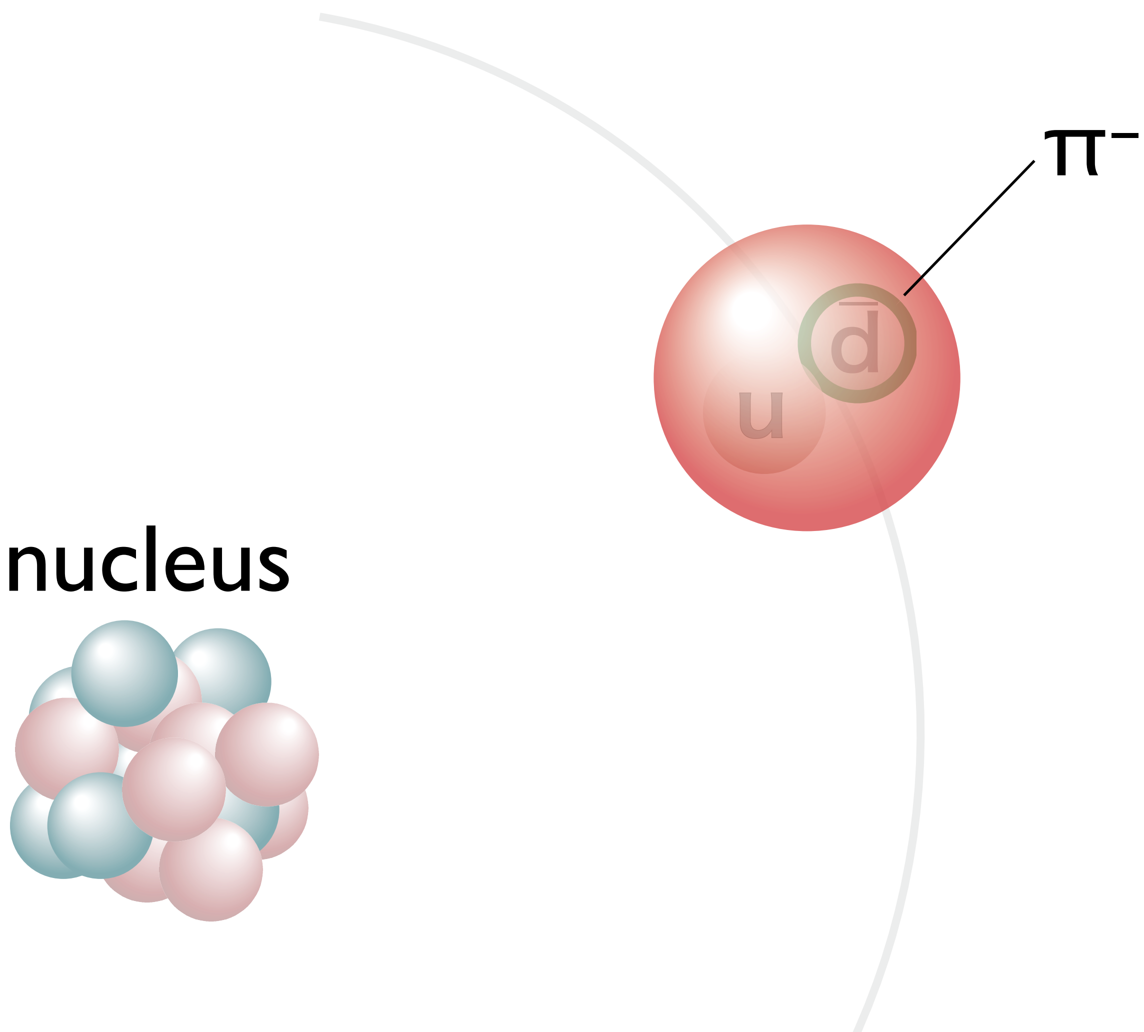

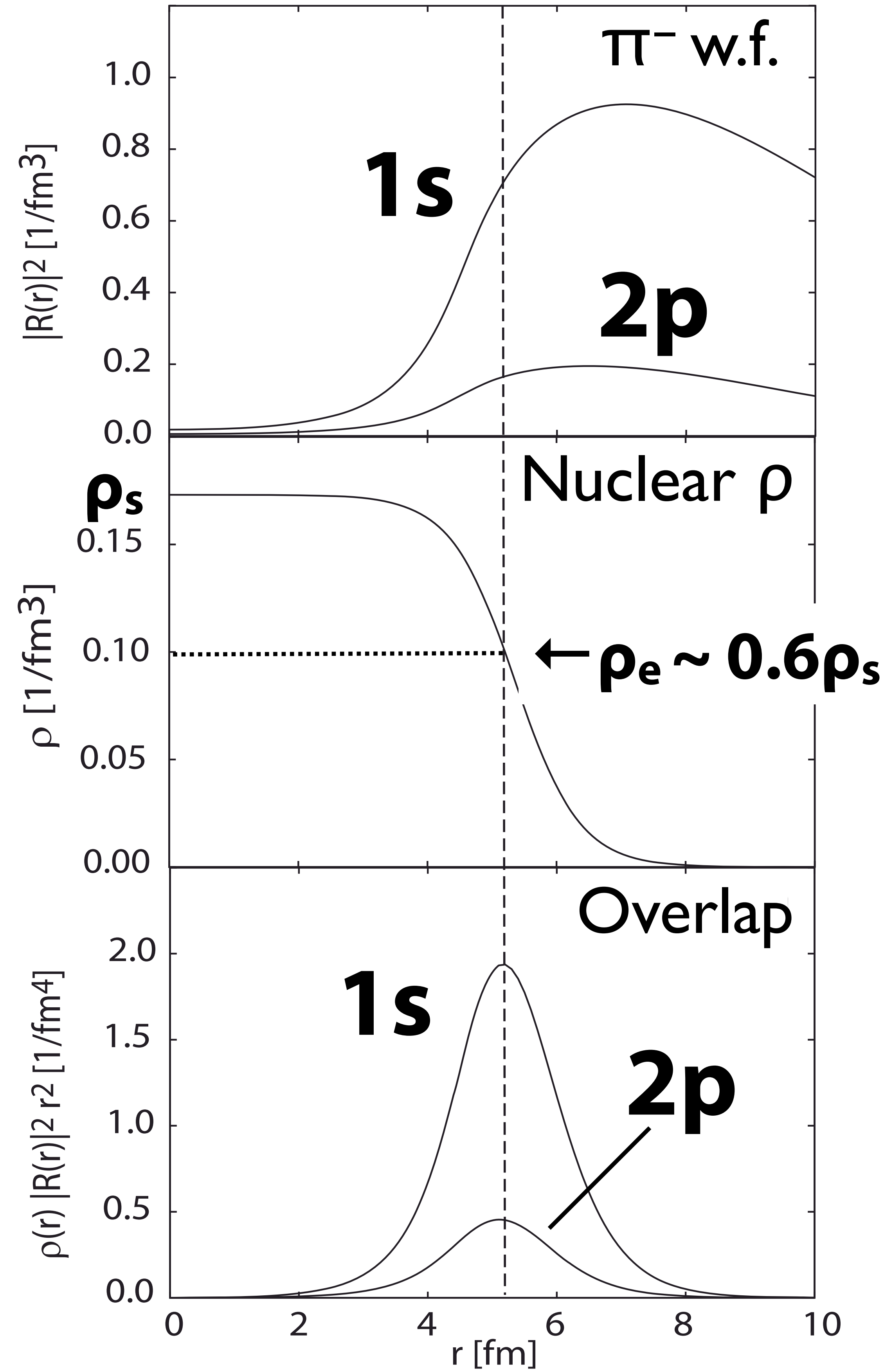

Ikeno et al., PTP126 (2011) 483

Ericson-Ericson potential

$$U_{\mathrm{opt}}(r) = U_s(r) + U_p(r),$$

$$U_s(r) = b_0\, \rho + \mathbf{b_1}\, (\rho_n - \rho_p) + B_0\, \rho^2$$

$$U_p(r) = \frac{2\pi}{\mu} \vec{\nabla} \cdot [c(r) + \varepsilon_2^{-1} C_0 \rho^2(r)] L(r) \vec{\nabla}$$

Pion-nucleus interaction

Overlap between
pion w.f. and nucleus
→ π works as a probe
at $\rho_e \sim 0.6\rho_s$

π-nucleus interaction is changed
for wavefunction renormalization
of medium effect

Ericson-Ericson potential

$$U_{\mathrm{opt}}(r) = U_s(r) + U_p(r),$$

$$U_s(r) = b_0\,\rho + \mathbf{b_1}\,(\rho_n - \rho_p) + B_0\,\rho^2$$

$$U_p(r) = \frac{2\pi}{\mu}\vec{\nabla}\cdot[c(r) + \varepsilon_2^{-1}C_0\rho^2(r)]L(r)\vec{\nabla}$$

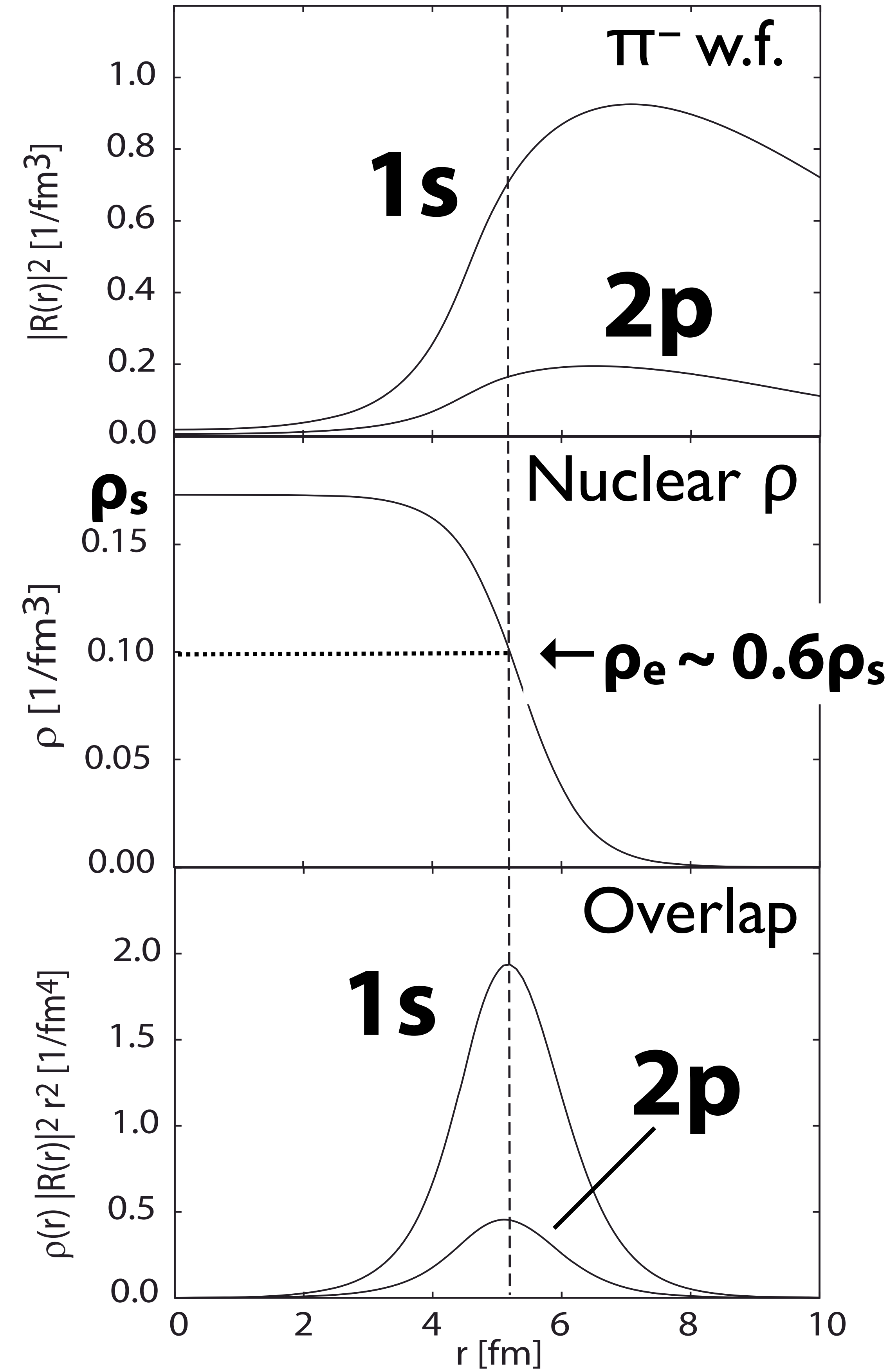

Ikeno et al., PTP126 (2011) 483

Pion-nucleus interaction and chiral condensate

Overlap between
pion w.f. and nucleus
→ π works as a probe
at $\rho_e \sim 0.6\rho_s$

π-nucleus interaction is changed
for wavefunction renormalization
of medium effect

Ericson-Ericson potential

$$U_{opt}(r) = U_s(r) + U_p(r),$$

$$U_s(r) = b_0\,\rho + \mathbf{b_1}\,(\rho_n - \rho_p) + B_0\,\rho^2$$

$$U_p(r) = \frac{2\pi}{\mu}\vec{\nabla}\cdot[c(r) + \varepsilon_2^{-1}C_0\rho^2(r)]L(r)\vec{\nabla}$$

In-medium Glashow-Weinberg relation

$$\frac{\langle\bar{q}q\rangle^*}{\langle\bar{q}q\rangle} \simeq \left(\frac{b_1^{\mathbf{v}}}{b_1}\right)^{1/2}\left(1-\gamma\,\frac{\rho}{\rho_0}\right)$$

$\gamma = 0.184 \pm 0.003$

Jido, Hatsuda, Kunihiro, PLB670, 109 (2008)

Pion-nucleus interaction and chiral condensate

Gell-Mann-Oakes-Renner relation

$$f_\pi^2 m_\pi^2 = -2m_q \langle \bar{q}q \rangle$$

Tomozawa-Weinberg relation

$$b_1 = -\frac{m_\pi}{8\pi f_\pi^2}$$

$$\frac{\langle \bar{q}q \rangle_\rho}{\langle \bar{q}q \rangle_0} \approx \frac{b_1^{\text{free}}}{b_1(\rho)}$$

M. Gell-Mann *et al.*, PR175(1968)2195.
Y. Tomozawa, NuovoCimA46(1966)707.
S. Weinberg, PRL17(1966)616.

In-medium Glashow-Weinberg relation

$$\frac{\langle \bar{q}q \rangle^*}{\langle \bar{q}q \rangle} \simeq \left(\frac{b_1^{\mathbf{v}}}{b_1}\right)^{1/2} \left(1 - \gamma \frac{\rho}{\rho_0}\right)$$

$\gamma = 0.184 \pm 0.003$

Jido, Hatsuda, Kunihiro, PLB670, 109 (2008)

High precision pionic hydrogen/deuterium measurement at PSI

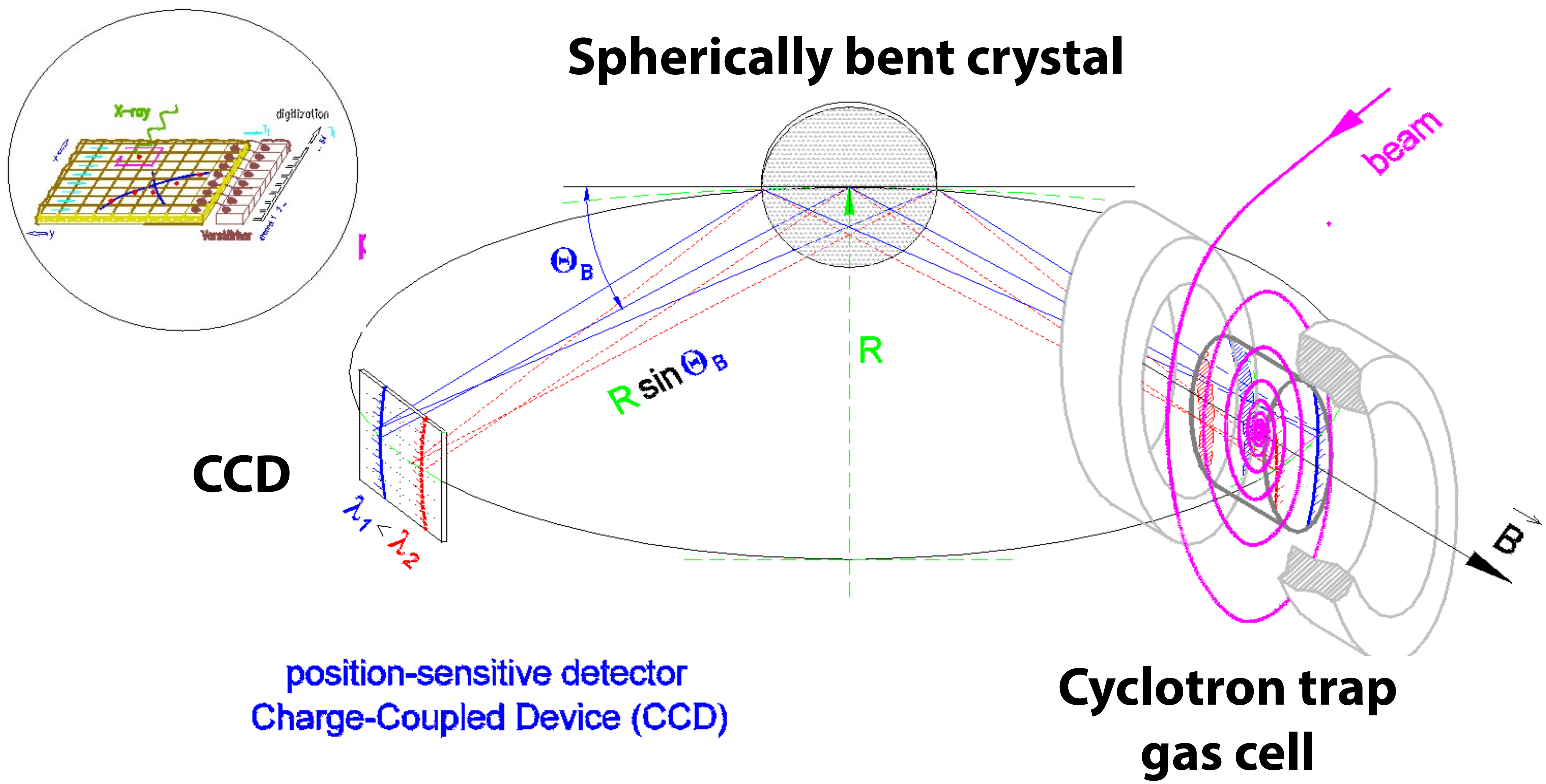

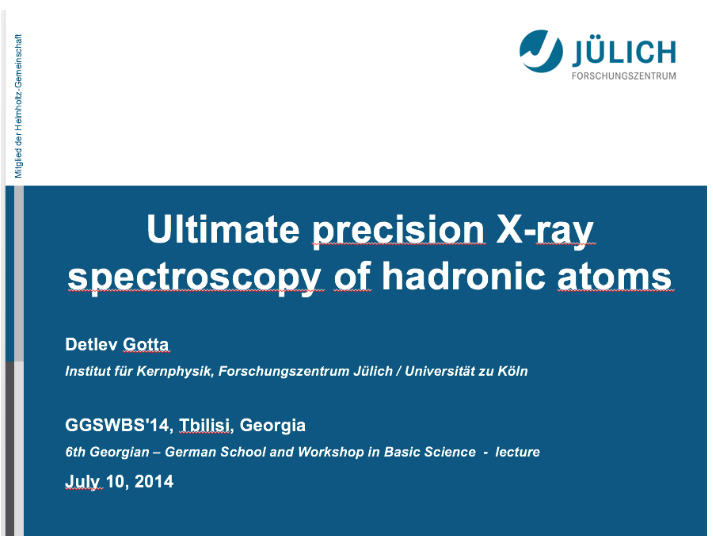
JÜLICH
FORSCHUNGSZENTRUM

Ultimate precision X-ray spectroscopy of hadronic atoms

Detlev Gotta

Institut für Kernphysik, Forschungszentrum Jülich / Universität zu Köln

GGSWBS'14, Tbilisi, Georgia

6th Georgian – German School and Workshop in Basic Science - lecture

July 10, 2014

Bragg reflection

$n\lambda = 2d \times \sin\theta_B$

High precision pionic hydrogen/deuterium measurement at PSI

X線凹面鏡

BRAGG CRYSTAL

Si 111

spherically curved

R = 3 m

Φ = 10 cm

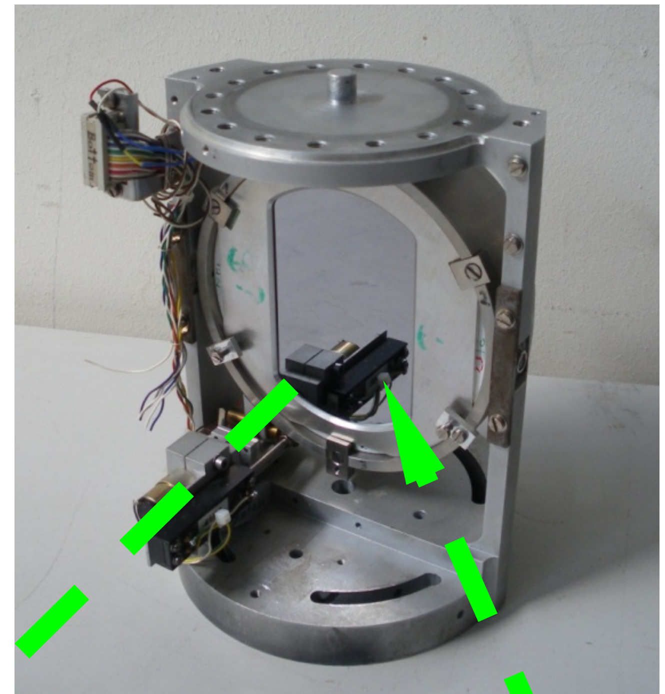

CCD検出器

Large - Area Focal Plane Detector

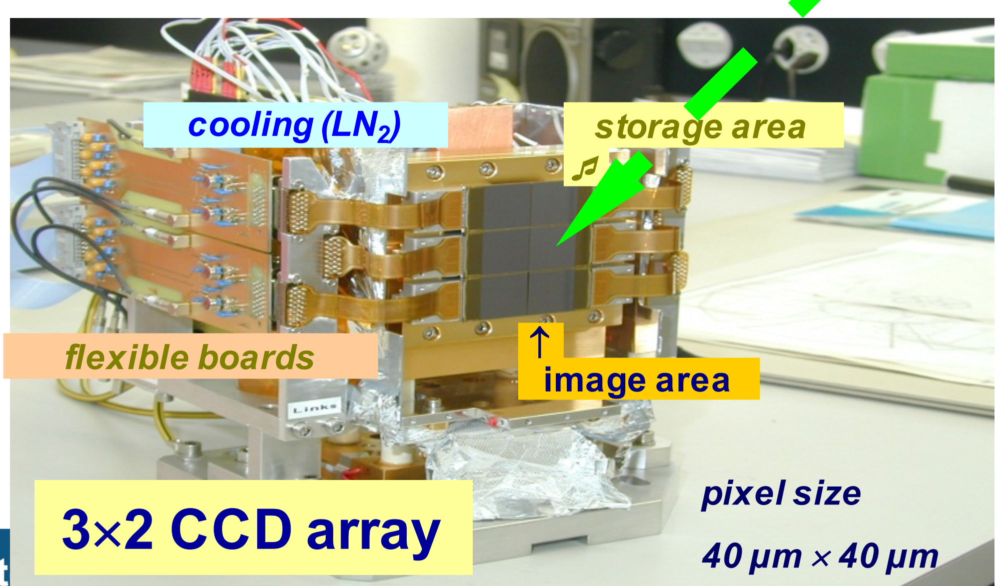

N. Nelms et al., Nucl. Instr. Meth 484 (2002) 419

CYCLOTRON TRAP

one coil removed

10^9 π/s

$\tau_{\pi\pm}$ = 26 ns

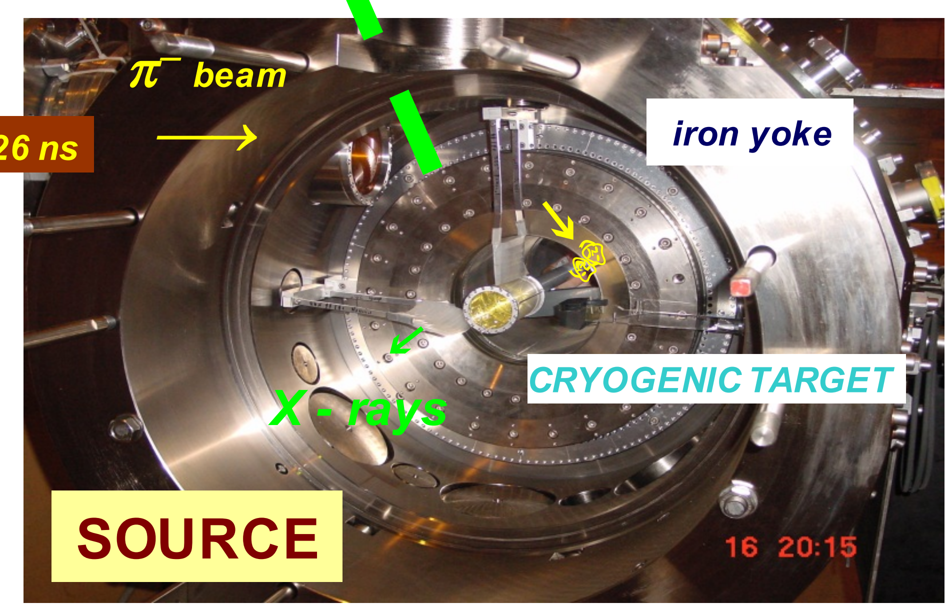

サイクロトロントラップ

see talk by M. Jabua

Pion-nucleus interaction and chiral condensate

Gell-Mann-Oakes-Renner relation

$$f_\pi^2 m_\pi^2 = -2 m_q \langle \bar{q} q \rangle$$

Tomozawa-Weinberg relation

$$b_1 = -\frac{m_\pi}{8\pi f_\pi^2}$$

$$\frac{\langle \bar{q} q \rangle_\rho}{\langle \bar{q} q \rangle_0} \approx \frac{b_1^{\mathrm{free}}}{b_1(\rho)}$$

In-medium Glashow-Weinberg relation

$$\frac{\langle \bar{q} q \rangle^*}{\langle \bar{q} q \rangle} \simeq \left(\frac{b_1^{\mathrm{v}}}{b_1} \right)^{1/2} \left(1 - \gamma \frac{\rho}{\rho_0} \right)$$

$\gamma = 0.184 \pm 0.003$

Jido, Hatsuda, Kunihiro, PLB670, 109 (2008)

Pionic hydrogen and deuterium

$b_1^{\mathrm{v}} = 0.0866 \pm 0.0010$

Hirtl et al., EPJA57, 70 (2021)

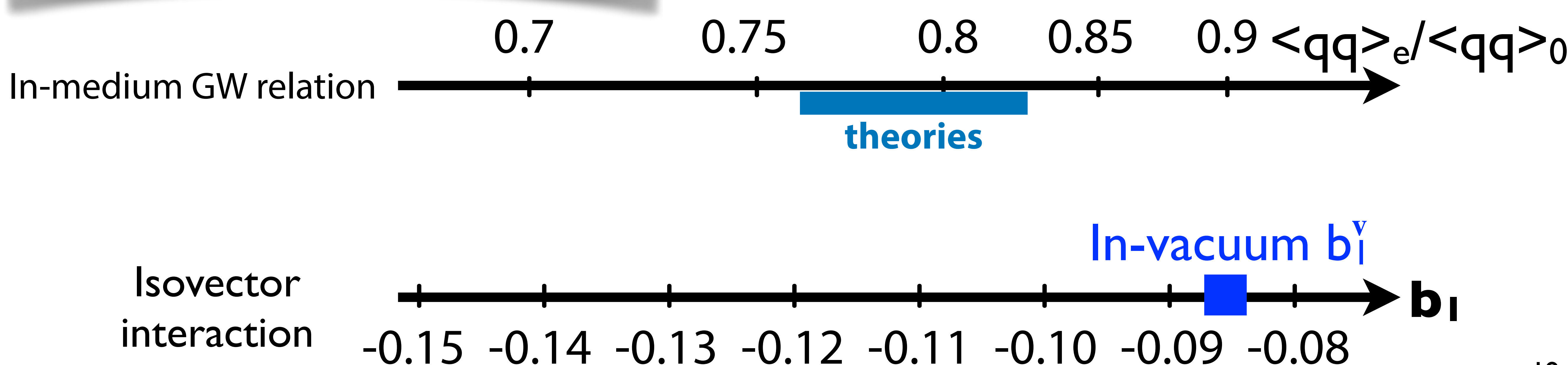

Level shifts in pionic X-ray measurements

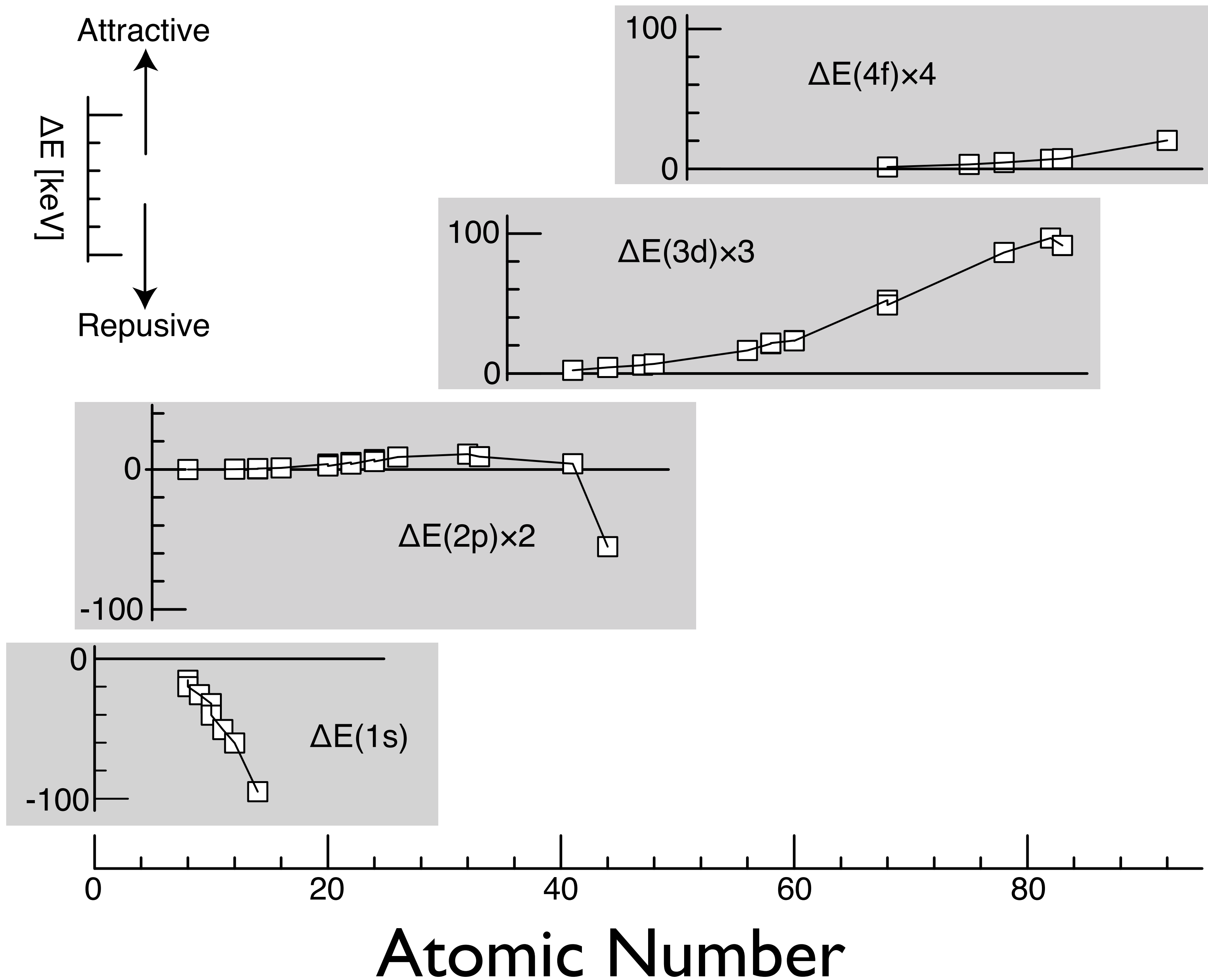

Ericson-Ericson potential

$$U_{\text{opt}}(r) = U_s(r) + U_p(r),$$

$$U_s(r) = b_0\,\rho + \mathbf{b_1}\,(\rho_n - \rho_p) + B_0\,\rho^2$$ ⟶ **s-wave = repulsive = negative shift**

$$U_p(r) = \frac{2\pi}{\mu}\vec{\nabla}\cdot[c(r) + \varepsilon_2^{-1}C_0\rho^2(r)]L(r)\vec{\nabla}$$ ⟶ **p-wave = attractive = positive shift**

Deeply bound pionic atoms
Level shifts

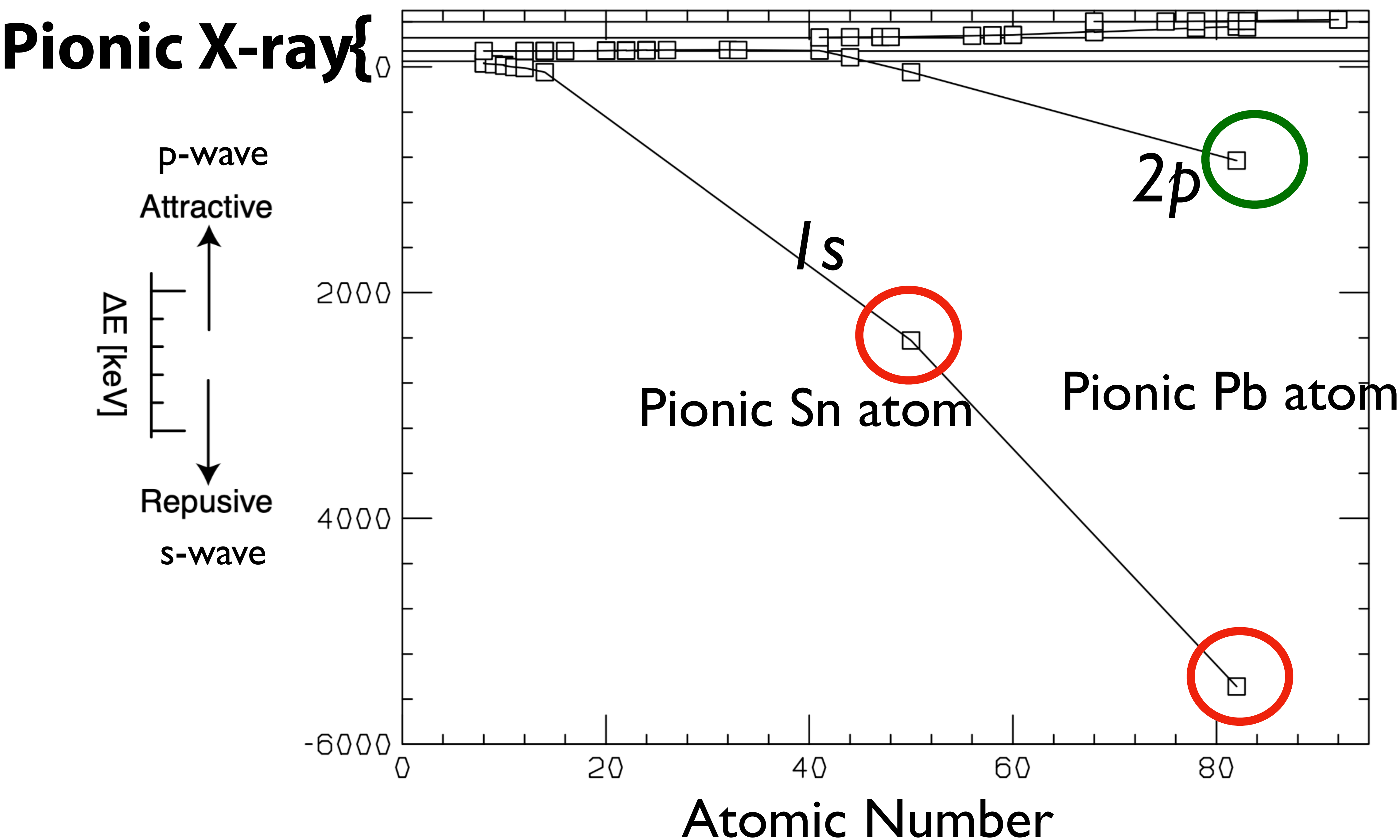

Deeply bound atoms have "super" repulsive shifts and provide *s*-wave information

piA and π-nucleus interaction

Deeply bound states
are sensitive to s-wave
cf. Pionic X-rays are to p-wave

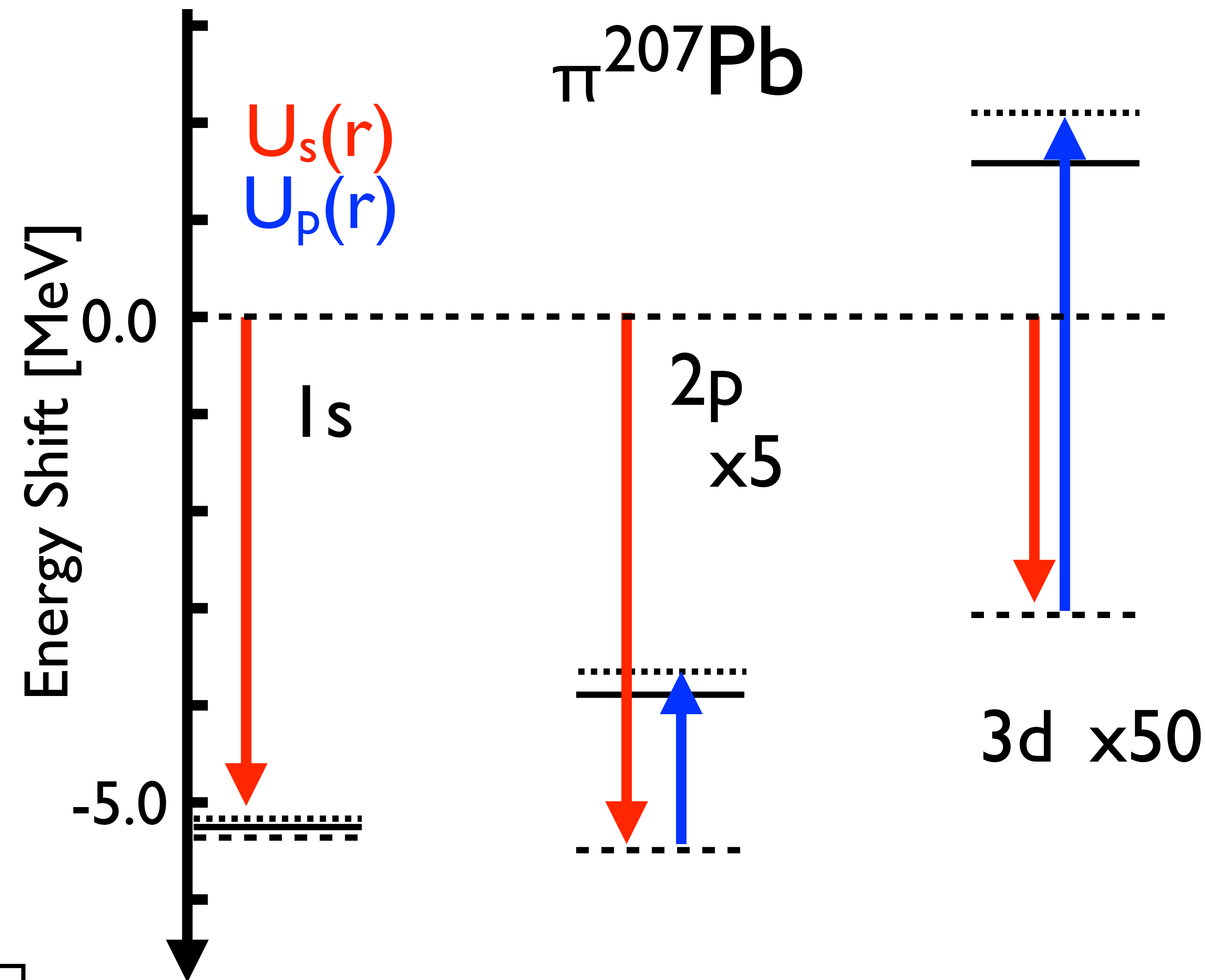

Ericson-Ericson potential

$$U_{\text{opt}}(r) = U_s(r) + U_p(r),$$

$$U_s(r) = b_0\,\rho + \mathbf{b_1}\,(\rho_n - \rho_p) + B_0\,\rho^2$$

$$U_p(r) = \frac{2\pi}{\mu}\vec{\nabla}\cdot[c(r) + \varepsilon_2^{-1}C_0\rho^2(r)]L(r)\vec{\nabla}$$

s-wave interaction is dominant in **1s shift**,
whereas p-wave is larger in 3d

PHYSICAL REVIEW C, VOLUME 62, 024606

Isotope dependence of deeply bound pionic states in Sn and Pb

Y. Umemoto,[1] S. Hirenzaki,[1] K. Kume,[1] and H. Toki[2]

Spectroscopy of pionic atoms in (d,^{3}He) reactions

Missing mass spectroscopy to measure excitation spectrum of pionic atoms

Direct production of pionic atoms

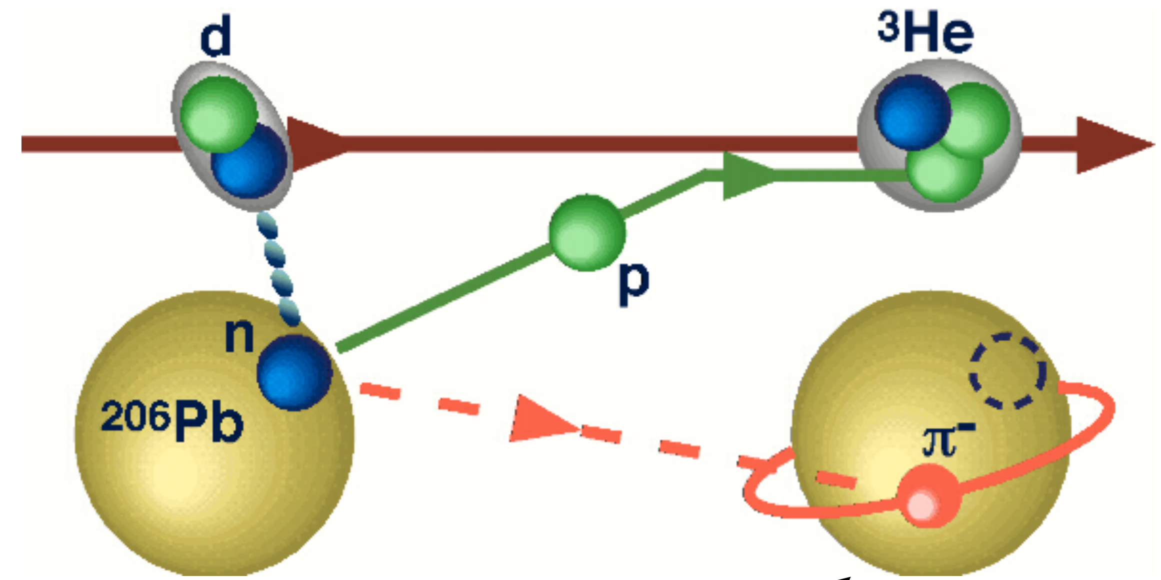

Momentum transfer

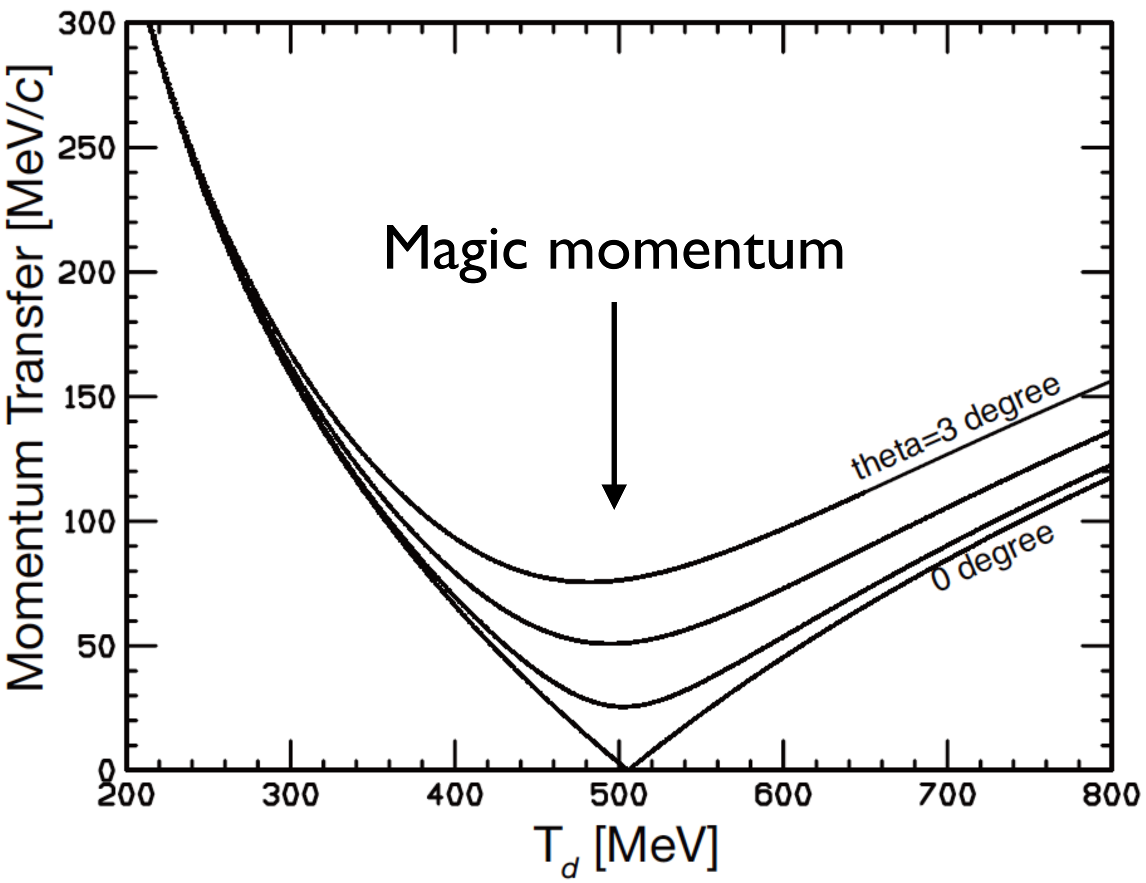

Pion bound state
(coupled with *n* hole)

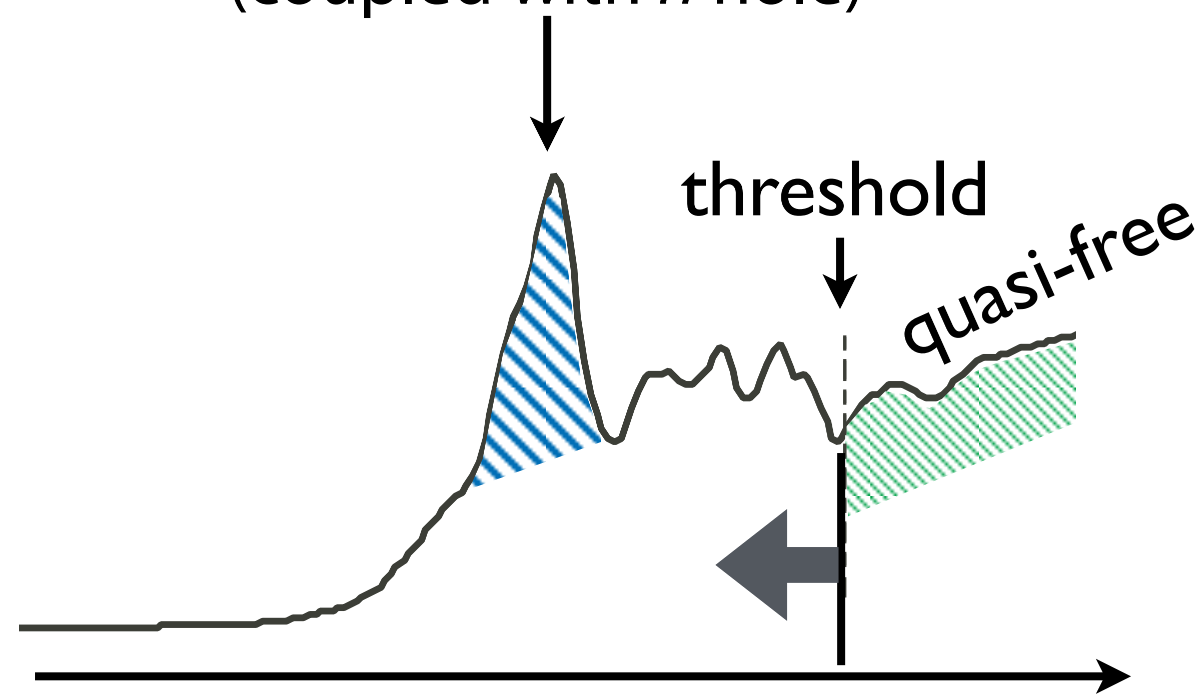

(d,³He) Reaction Spectroscopy in RIBF

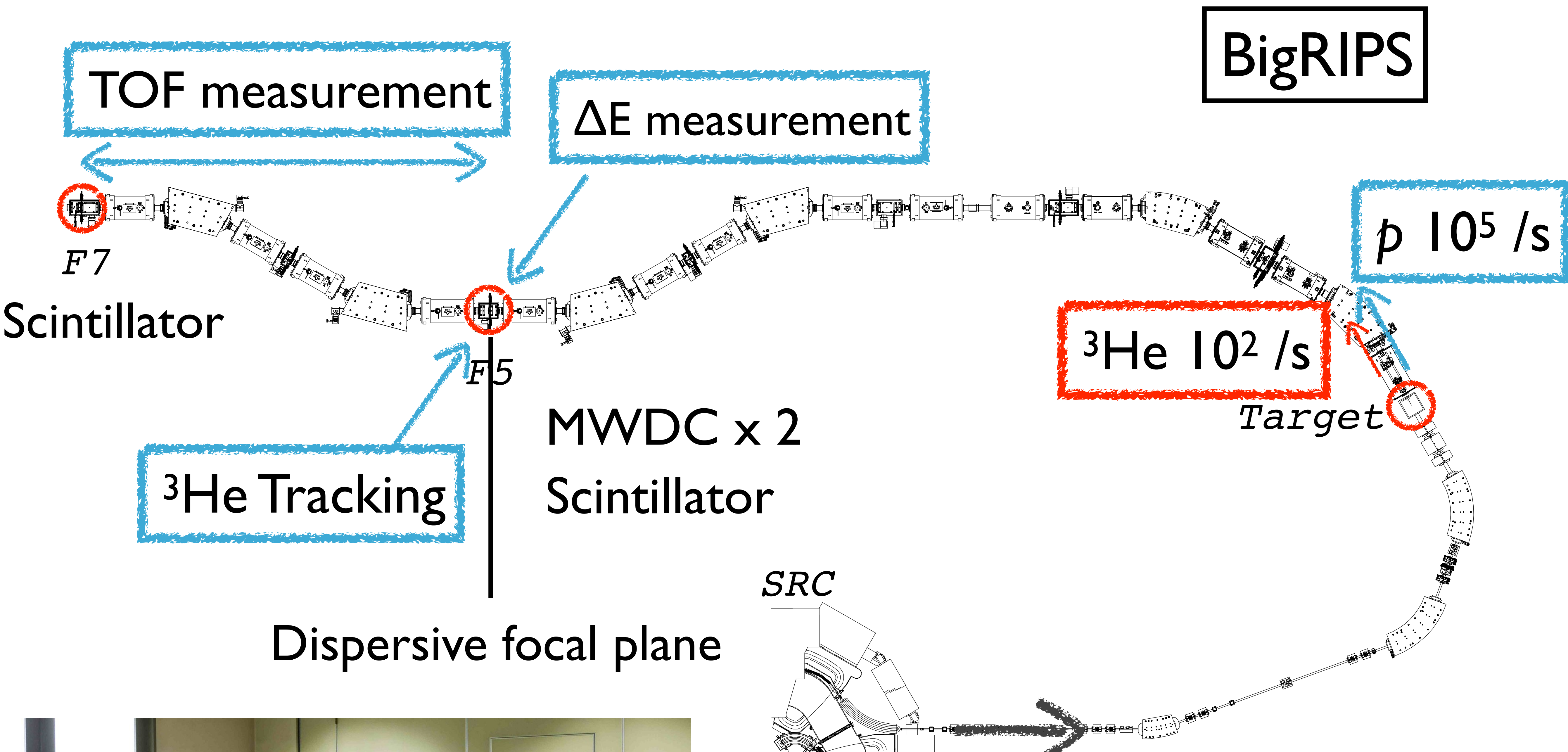

d beam >10¹² /s, 500 MeV

tahashi, RIKEN

Reaction spectroscopy of pionic atom

Search for pionic atoms GSI-S160	1996	$^{208}Pb(d,^{3}He)$
1s measurement GSI-S160	1998	$^{206}Pb(d,^{3}He)$
Systematic run with Sn GSI-S236	2002	$^{116\text{-}124}Sn(d,^{3}He)$
Pilot run at RIBF RIBF-27	**2010**	$^{122}Sn(d,^{3}He)$
Production RIBF-54R1	**2014**	$^{117,122}Sn(d,^{3}He)$
Systematic Measurement RIBF-135	2021	$^{112\text{-}124}Sn(d,^{3}He)$
Inverse (pilot) RIBF-214		$D(^{136}Xe,^{3}He)$
Inverse		$D(X, ^{3}He)$

(p,2He), (p,2p) in RCNP

RI Beam Factory

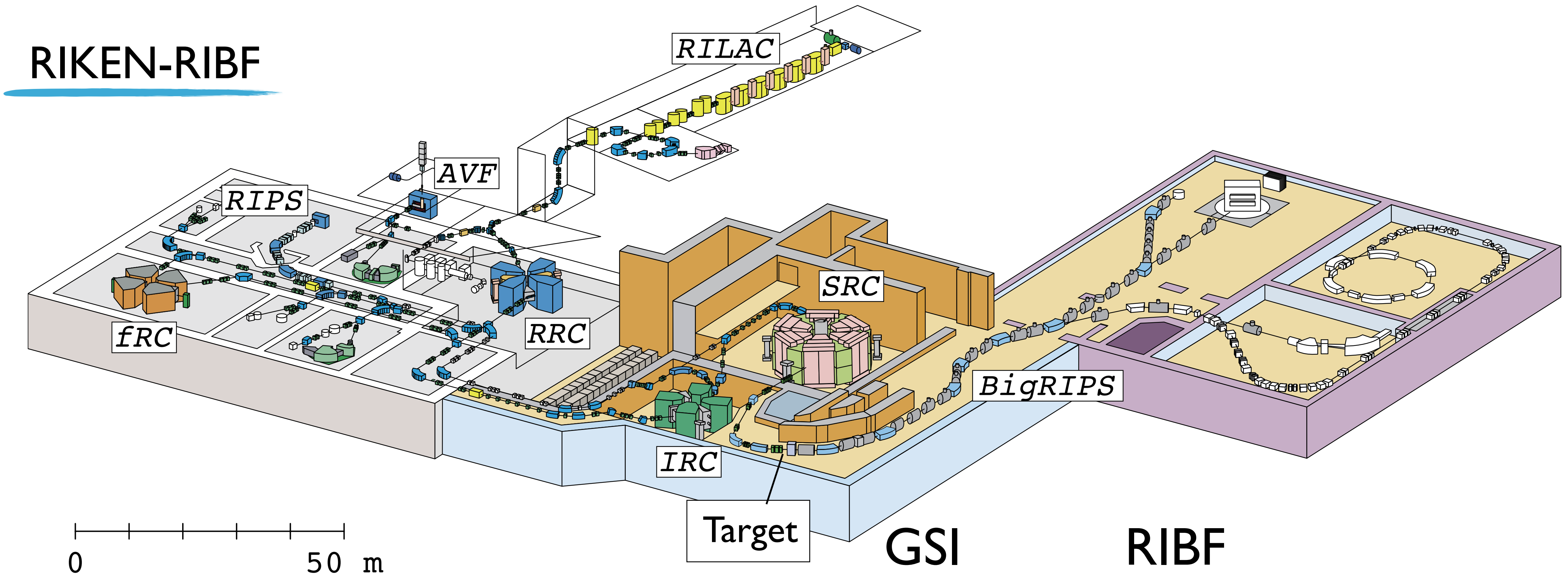

	GSI	RIBF
d beam Intensity	10^{11}/spill	>10^{12}/s
Target	20 mg/cm^2	10 mg/cm^2
$\Delta p_d/p_d$ (FWHM)	0.02%	0.06%
Resolution (FWHM)	400 keV	~1000 keV
Acceptance (mrad)	15H, 10V	40H, 60V

RIKEN NiSHiNA CENTER

Kenta Itahashi, RIKEN

RI Beam Factory

RIKEN-RIBF

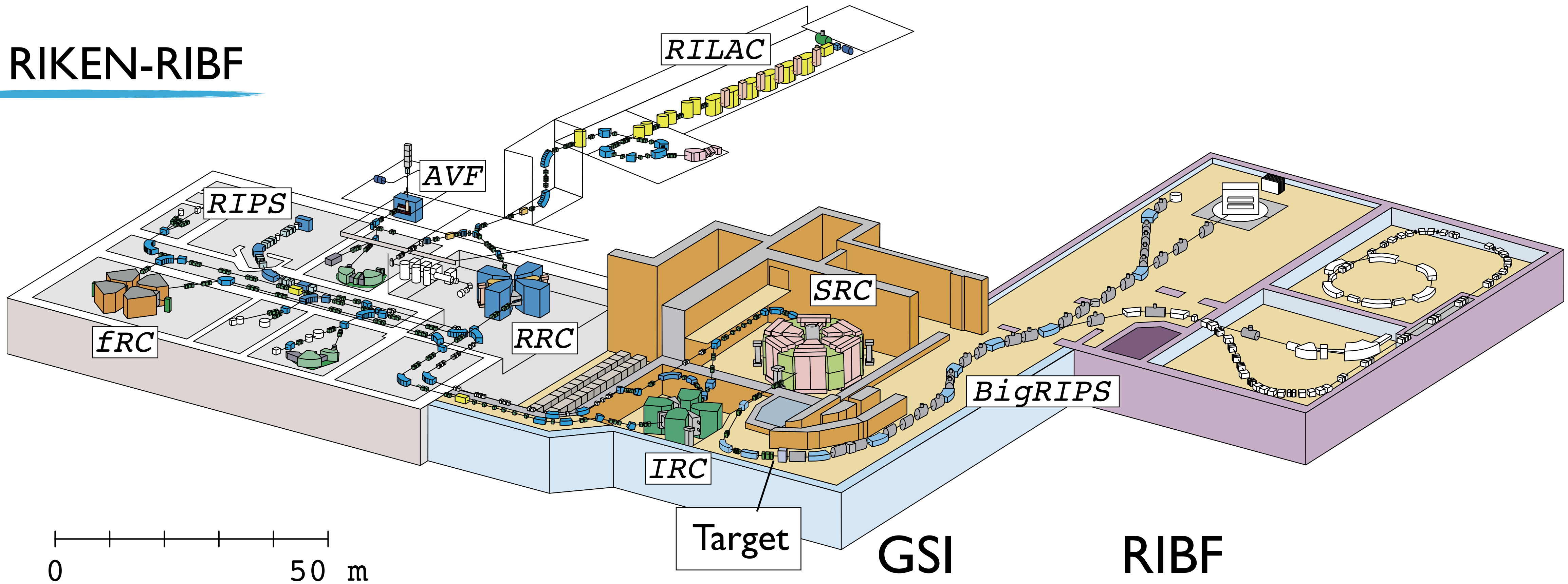

	GSI	RIBF
d beam Intensity	10^{11}/spill	>10^{12}/s
Target	20 mg/cm^2	10 mg/cm^2
$\Delta p_d/p_d$ (FWHM)	0.02%	0.06%
Resolution (FWHM)	400 keV	~300 keV
Acceptance (mrad)	15H, 10V	40H, 60V

Dispersion matching

RIKEN NiSHiNA CENTER

Kenta Itahashi, RIKEN

Resolution improvement technique

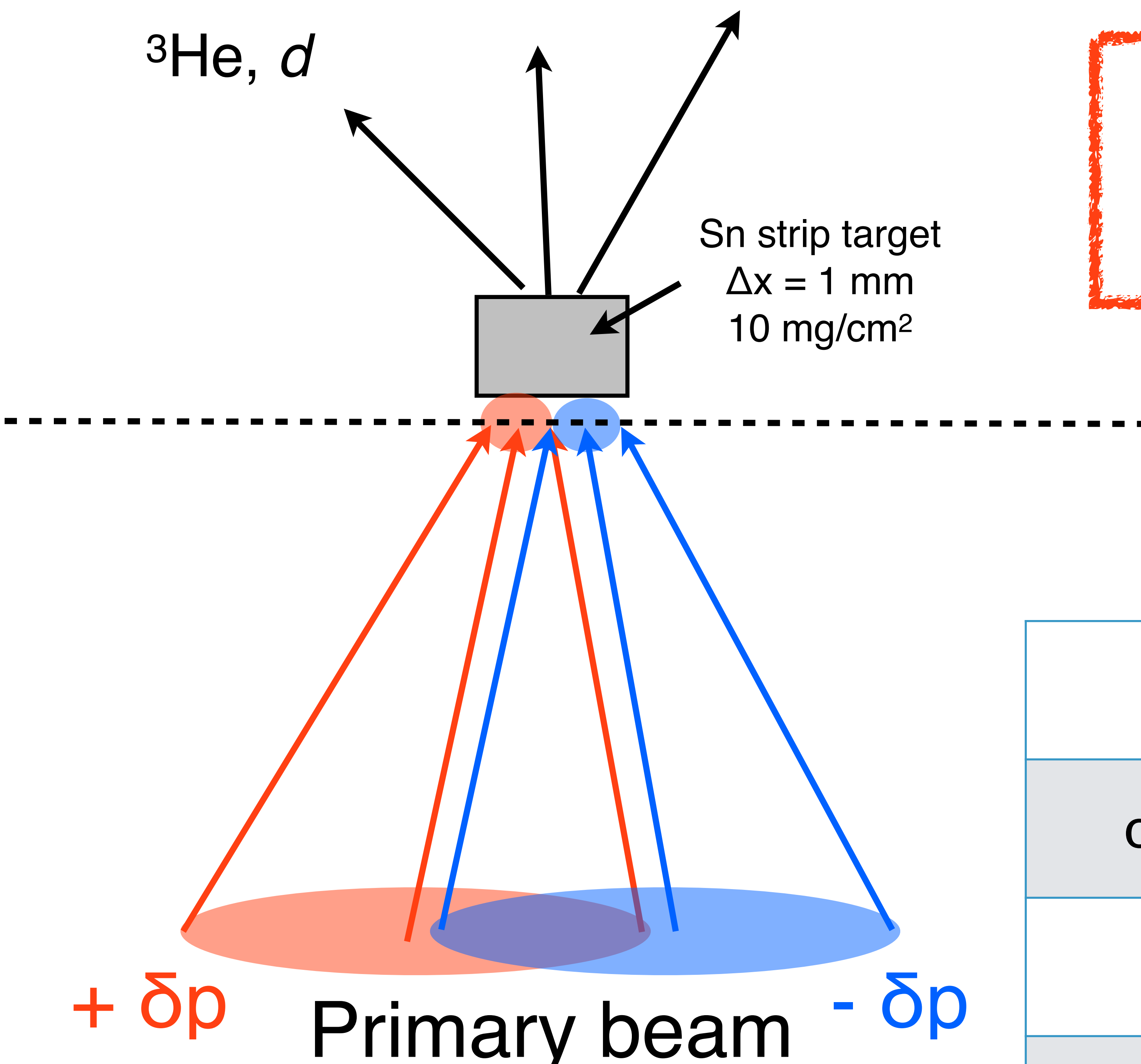

Dispersion matching

Analysis of beam energy in the beam line

← F0 (dispersive target position)
45 mm/%

	pilot (2010)	2014
$\sigma p_{primary}$ [%]	0.04	0.03
σx_{F0} [mm]	0.7	**0.2**
$resolution_{exp}$ [keV]	500	**280**

Resolution improvement technique

Dispersion matching using primary beam

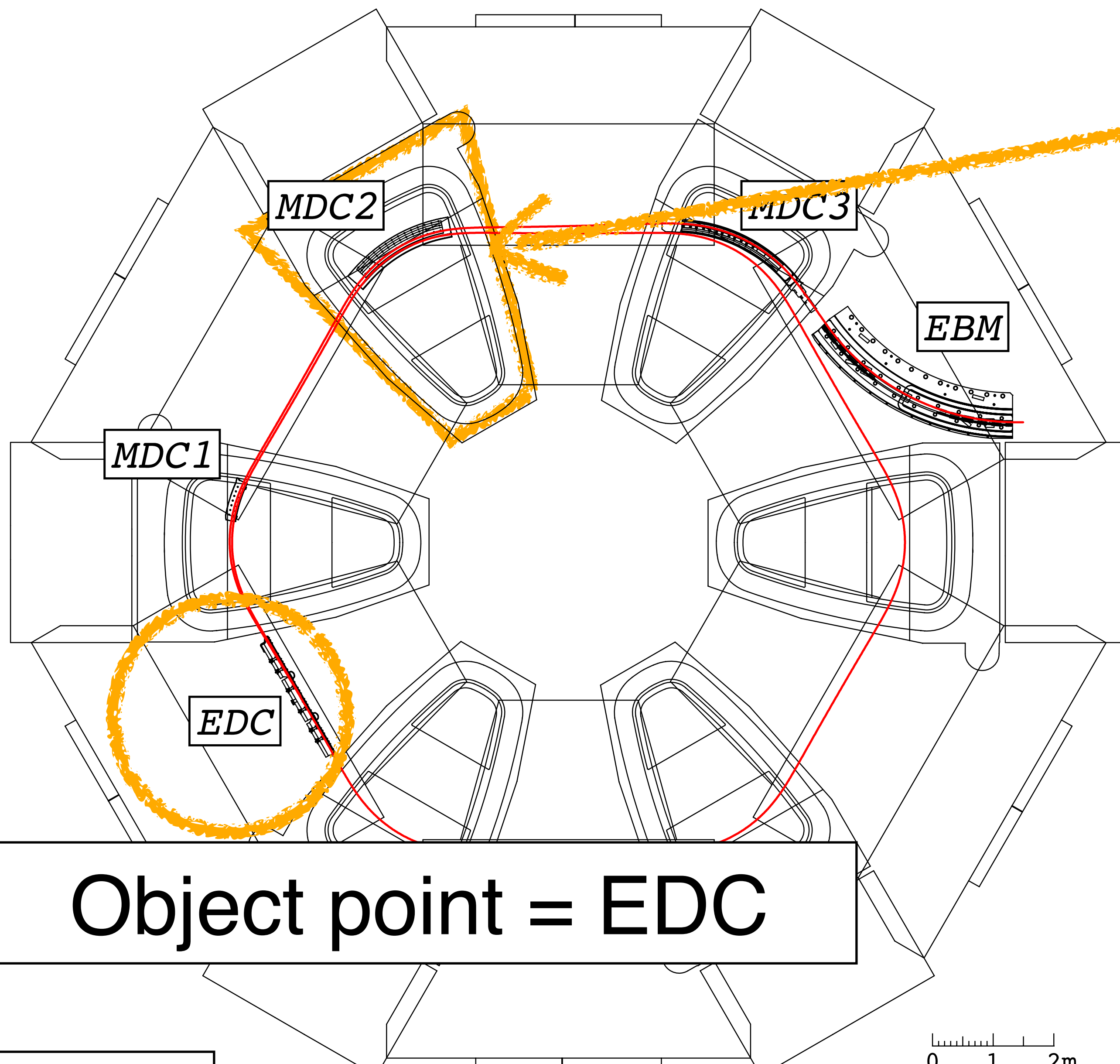

Object point = EDC

SRC

magnetic field in the magnet

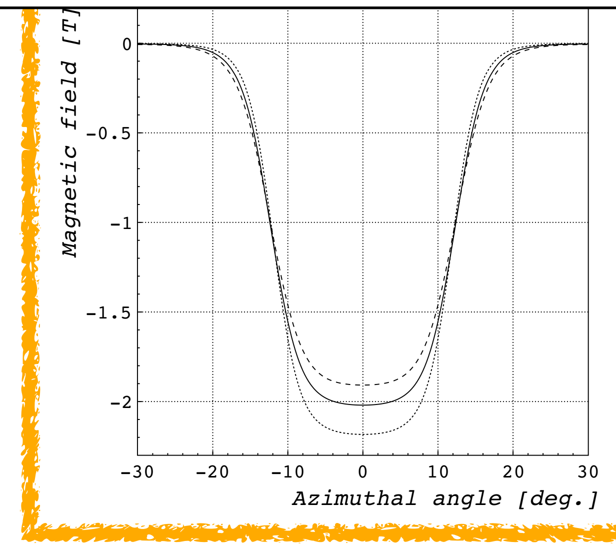

calculate the transfer matrix using Runge-Kutta method

$$
\begin{pmatrix}
(x|x) & (x|a) & (x|y) & (x|b) & (x|\delta) \\
(a|x) & (a|a) & (a|y) & (a|b) & (a|\delta) \\
(y|x) & (y|a) & (y|y) & (y|b) & (y|\delta) \\
(b|x) & (b|a) & (b|y) & (b|b) & (b|\delta)
\end{pmatrix}_{\mathrm{EDC}\rightarrow\mathrm{EBM}}
=
\begin{pmatrix}
-1.00 & -3.35 & 0.0 & 0.0 & 76.9 \\
0.30 & -0.01 & 0.0 & 0.0 & -25.4 \\
0.0 & 0.0 & -1.03 & -1.75 & 0.0 \\
0.0 & 0.0 & -0.09 & -1.12 & 0.0
\end{pmatrix}
$$

Resolution improvement technique

Beam Transfer line

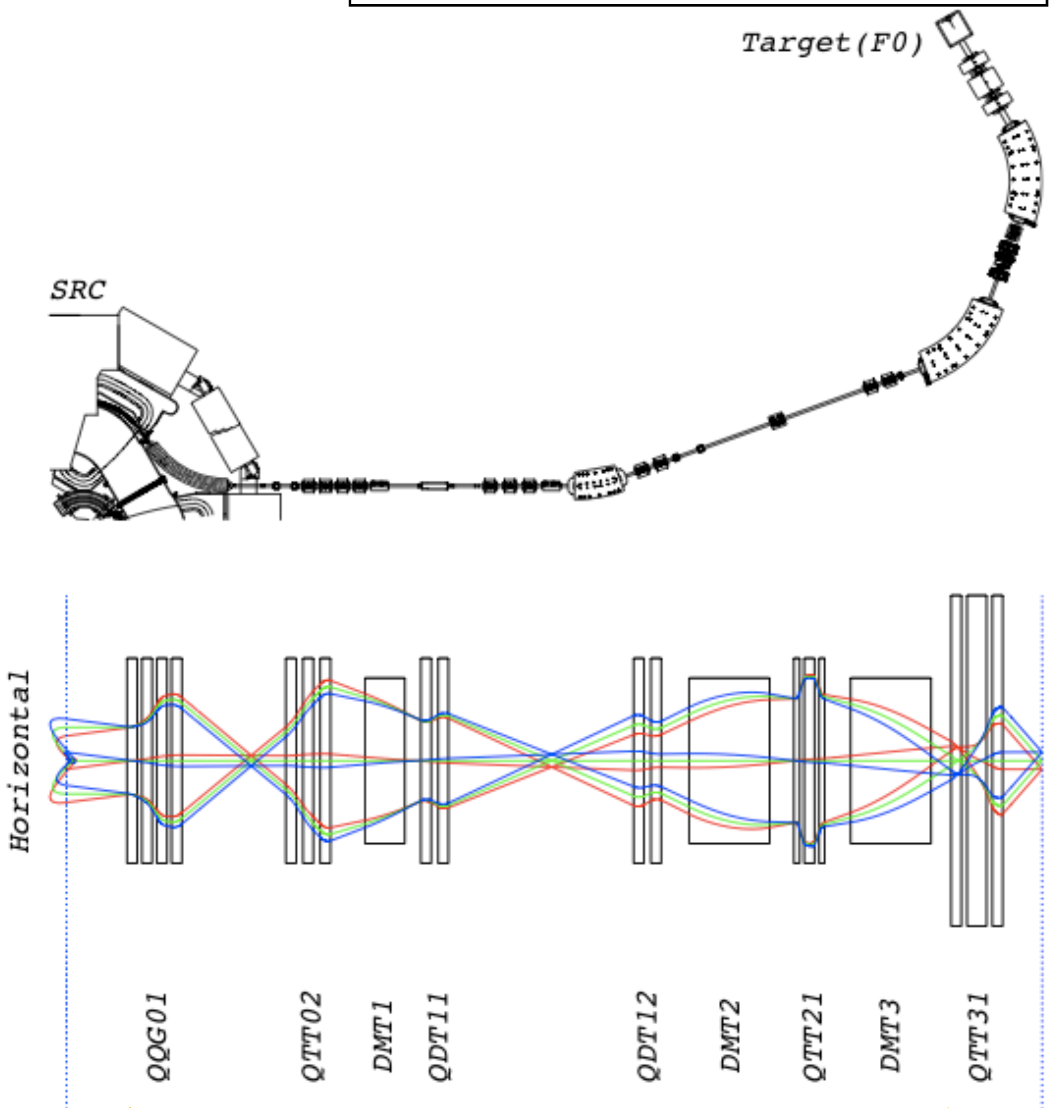

dispersion matching

BigRIPS

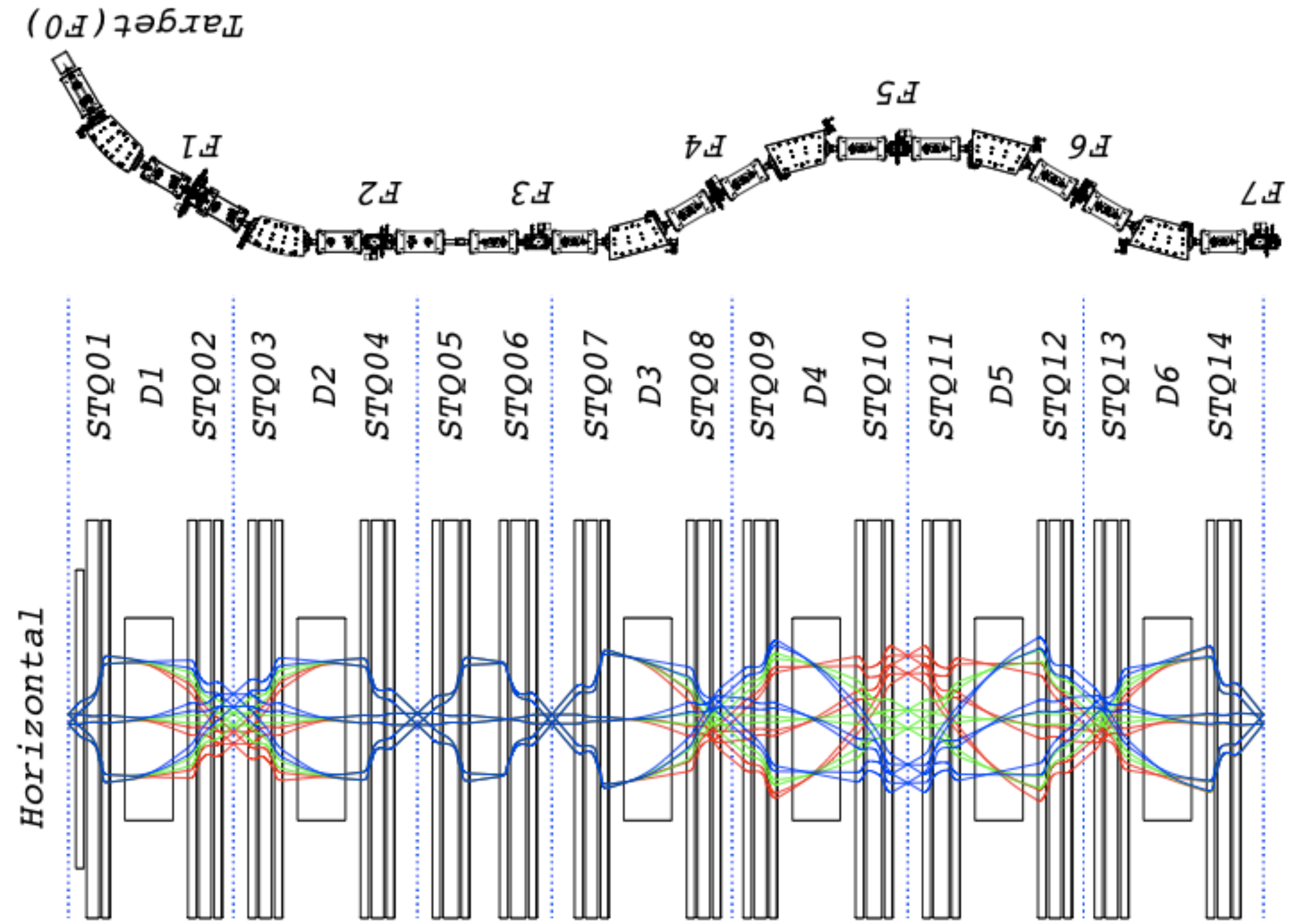

Q analysis

pID

dispersion: 62 mm/%

<u>Measured observable (= position at focal plane) reflects only Q-value</u>

T. Nishi et al.: Nucl. Instrum. Methods. in Phys. Res. B 317 290-293 (2013)

Resolution estimation

FWHM [keV]	2014	2021
Target thickness	110	30
Multiple scattering	120	45
Beam & optics	200	85
Total	**~280**	**~100?**

cf. 400 keV in GSI and in 2010

Pionic ^{121}Sn atom

Pilot run

15 hours DAQ in 2010

First observation of θ dependence of π atom cross section

$\Delta L \sim R \times q$

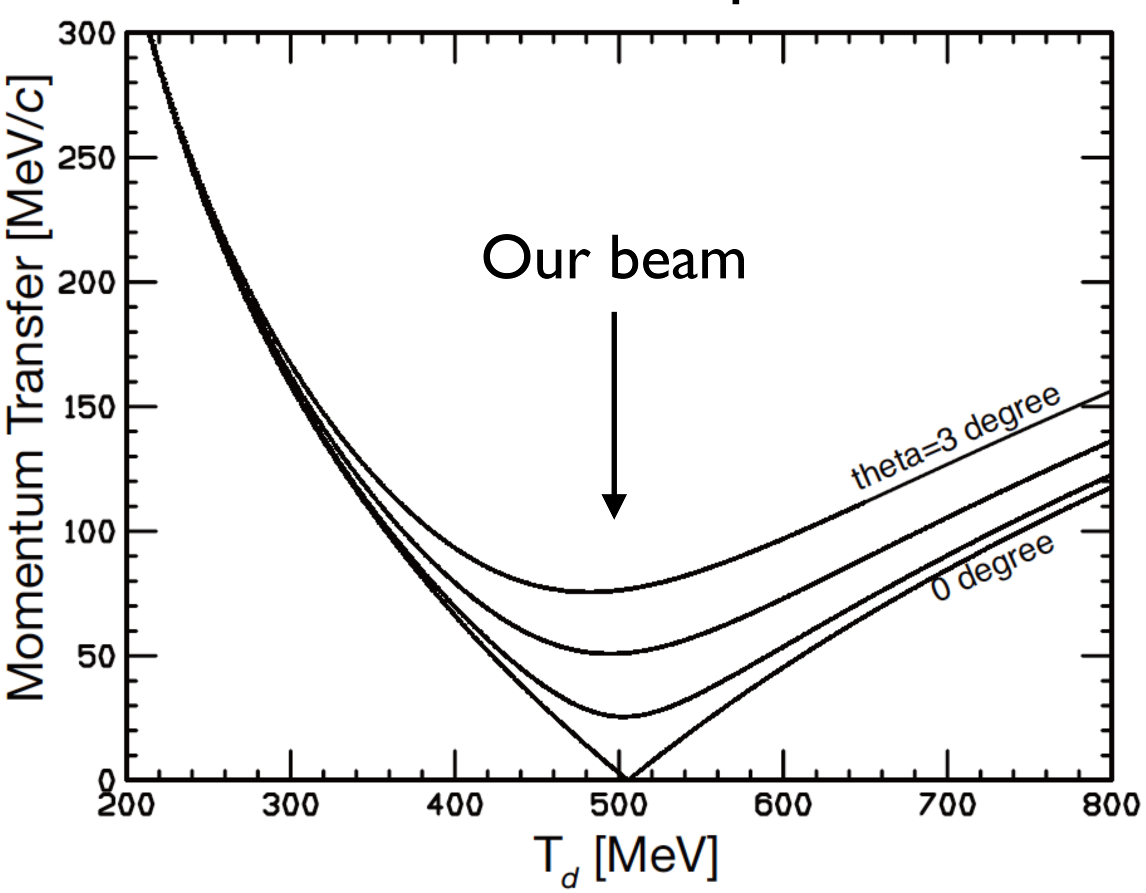

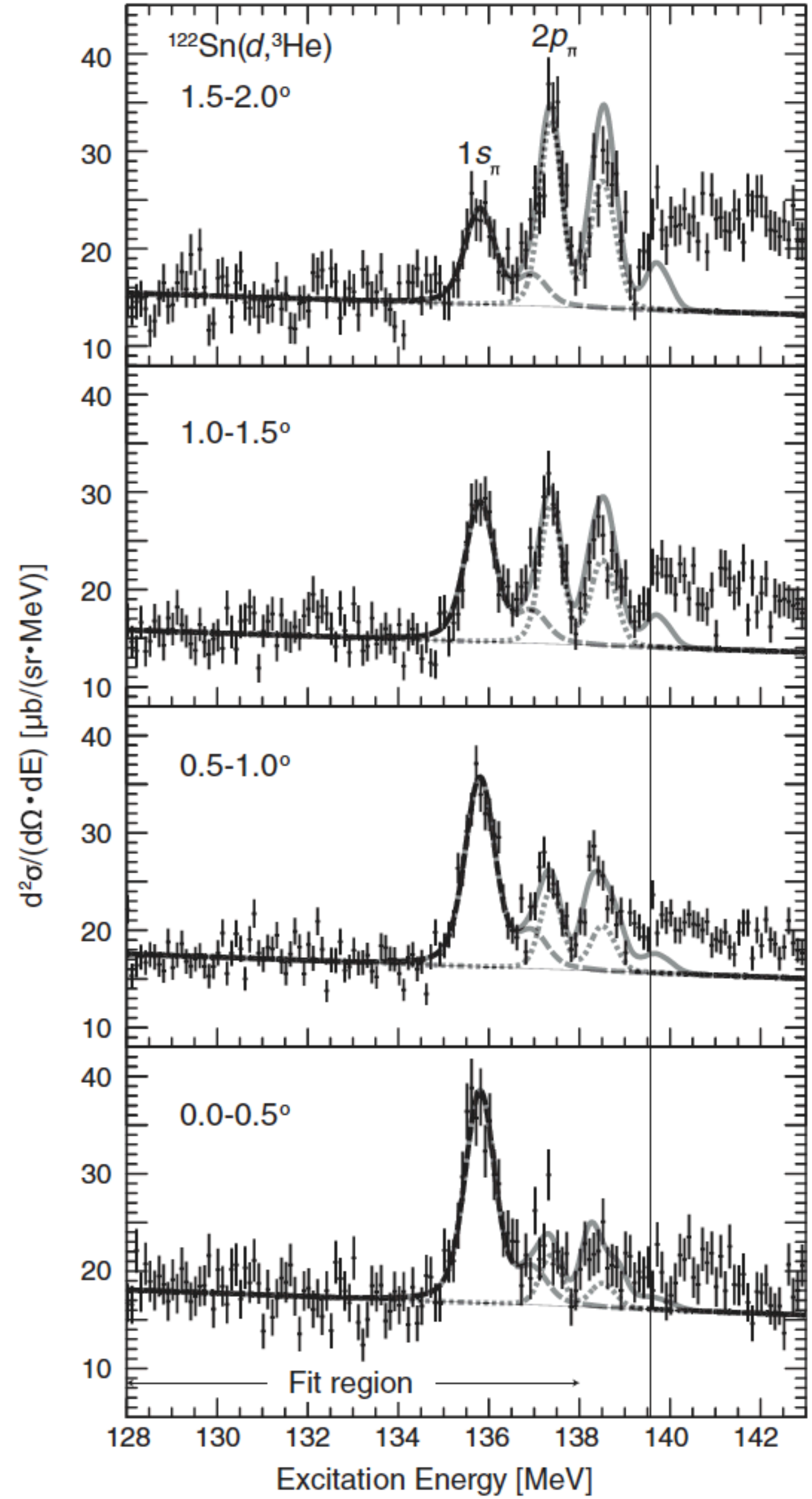

T. Nishi KI et al., PRL120, 152505 (2018)

1s and 2p pionic atom cross sections in (d,³He)

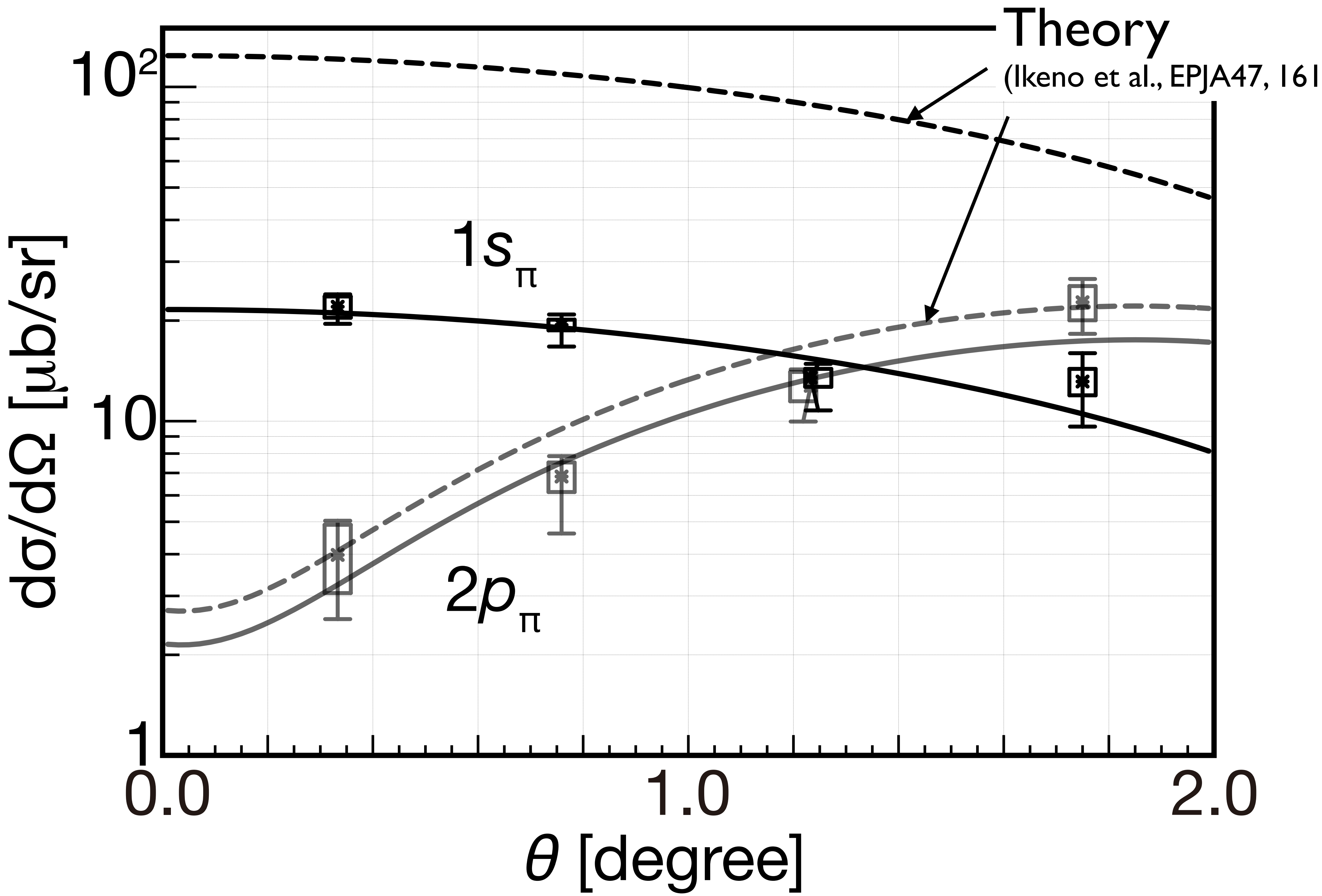

θ dependence is well reproduced.
Theory calculates 5x larger cross section for 1s

T. Nishi KI et al., PRL120, 152505 (2018)

T. Nishi KI et al., PRL120, 152505 (2018)

Pionic ^{121}Sn atom

Pilot run

15 hours DAQ in 2010

First simultaneous 1s and 2p observation

$$B_{1s} = 3.828 \pm 0.013(\mathrm{stat})^{+0.036}_{-0.033}(\mathrm{syst})\ \mathrm{MeV}$$
$$\Gamma_{1s} = 0.252 \pm 0.054(\mathrm{stat})^{+0.053}_{-0.070}(\mathrm{syst})\ \mathrm{MeV}$$
$$B_{2p} = 2.238 \pm 0.015(\mathrm{stat})^{+0.046}_{-0.043}(\mathrm{syst})\ \mathrm{MeV}$$

Resolution 394 keV (FWHM)

Theories

B_{1s}= 3.787–3.850 MeV

Γ_{1s}= 0.306–0.324 MeV

B_{2p}= 2.257–2.276 MeV

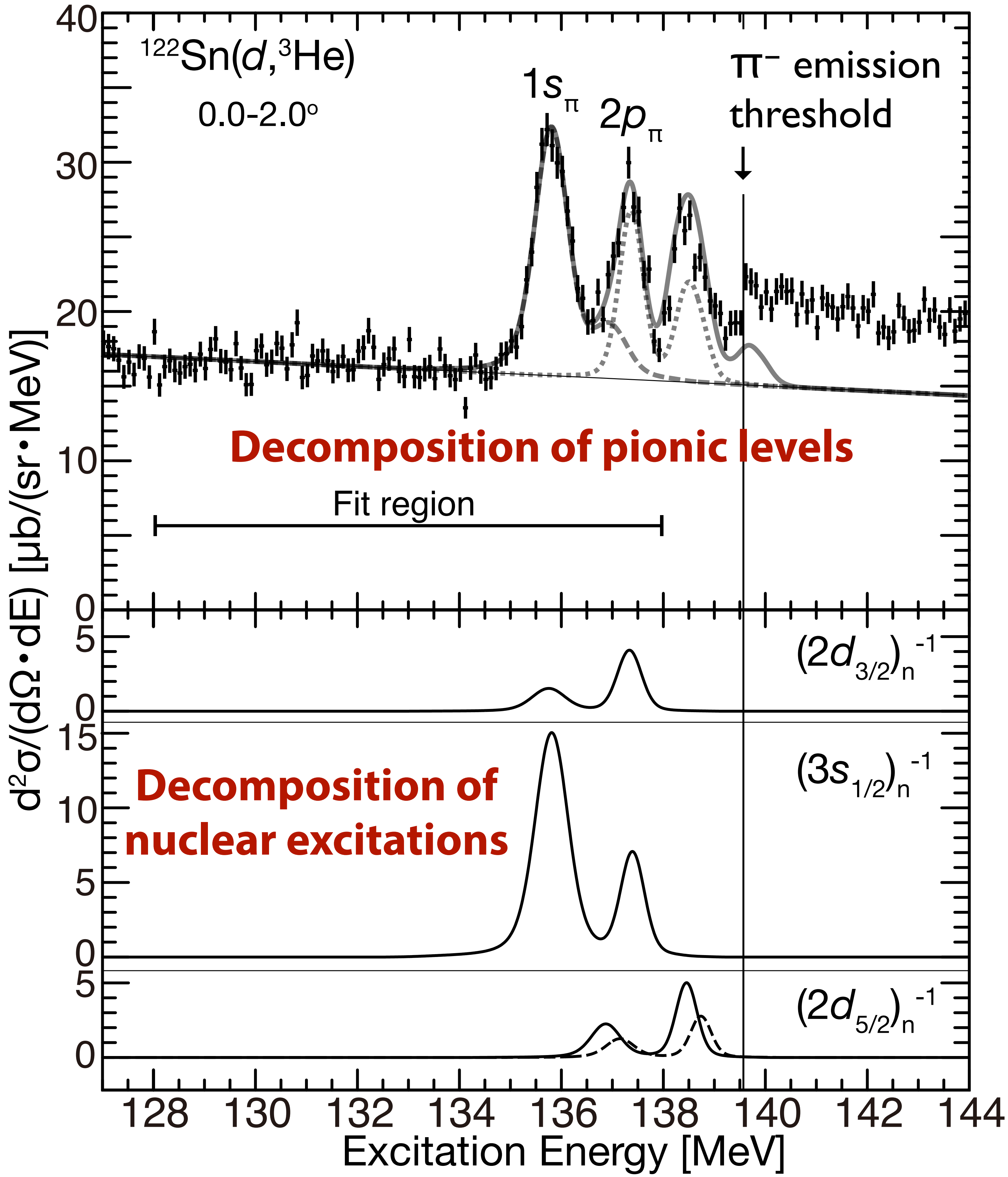

T. Nishi KI et al., PRL120, 152505 (2018)

Pionic ^{121}Sn atom

Pilot run

15 hours DAQ in 2010

First simultaneous 1s and 2p observation

$B_{1s} = 3.828 \pm 0.0$ …

$\Gamma_{1s} = 0.252 \pm 0.0$ … $_{-0.070}$ … MeV

$B_{2p} = 2.238 \pm 0.015(\mathrm{stat})^{+0.046}_{-0.043}(\mathrm{syst})$ MeV

Resolution 394 keV (FWHM)

Theories

B_{1s}= 3.787–3.850 MeV

Γ_{1s}= 0.306–0.324 MeV

B_{2p}= 2.257–2.276 MeV

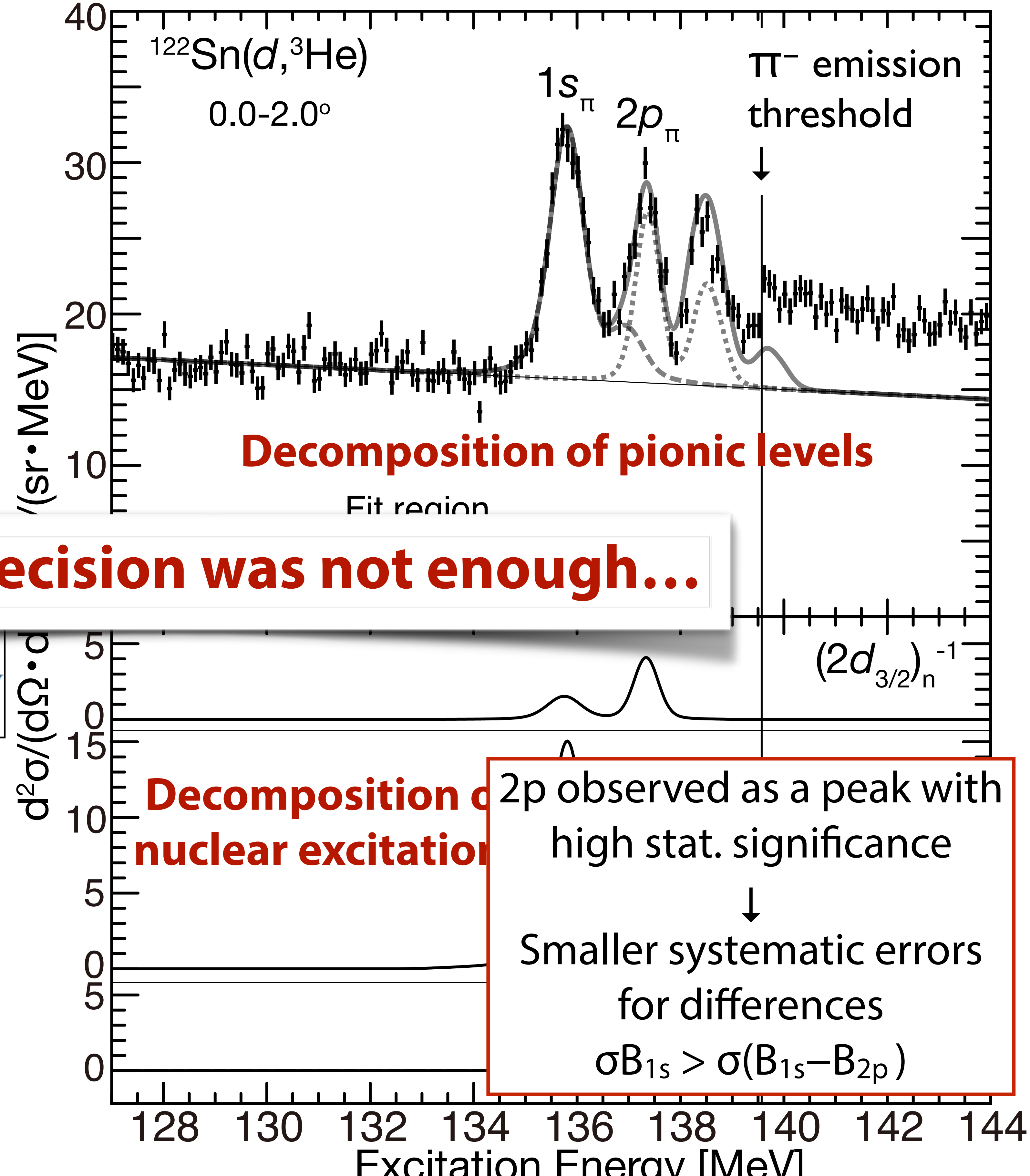

However, precision was not enough…

2p observed as a peak with high stat. significance

↓

Smaller systematic errors for differences

$\sigma B_{1s} > \sigma(B_{1s} - B_{2p})$

Measured nuclear density distribution of Sn isotopes
Sn(p,p') reaction at RCNP, Osaka

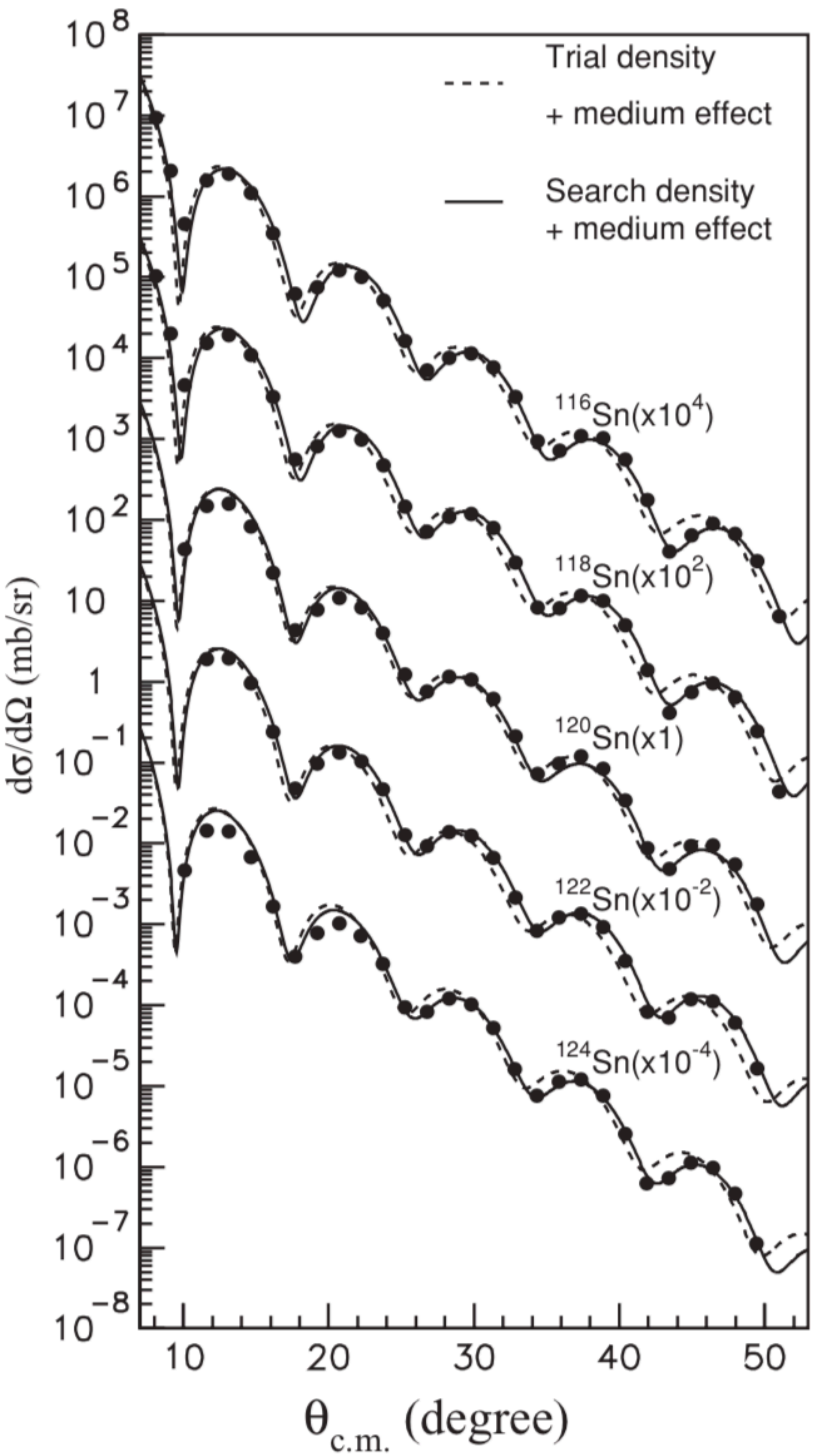

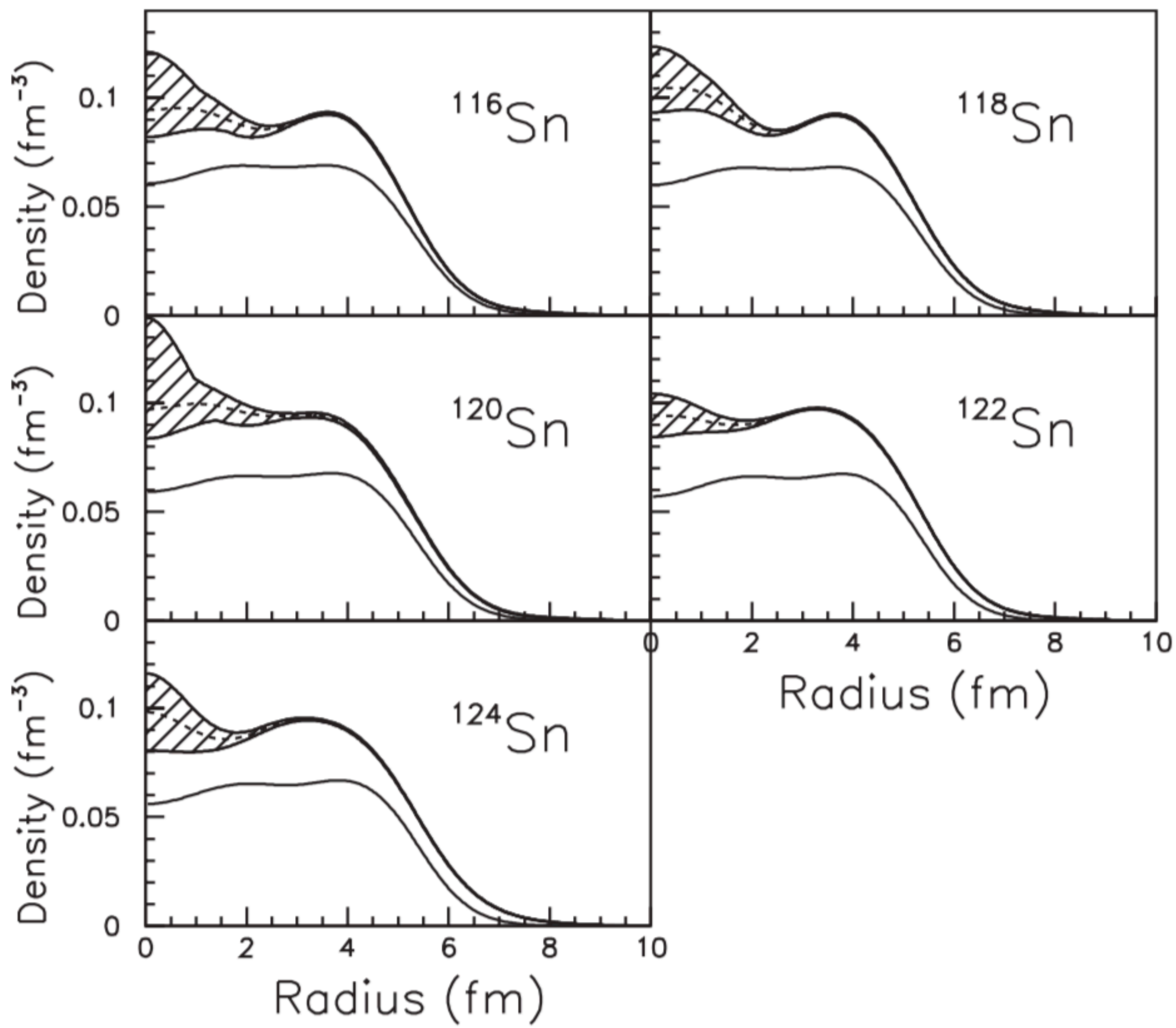

Terashima et al., PHYSICAL REVIEW C **77**, 024317 (2008)

Residual interaction

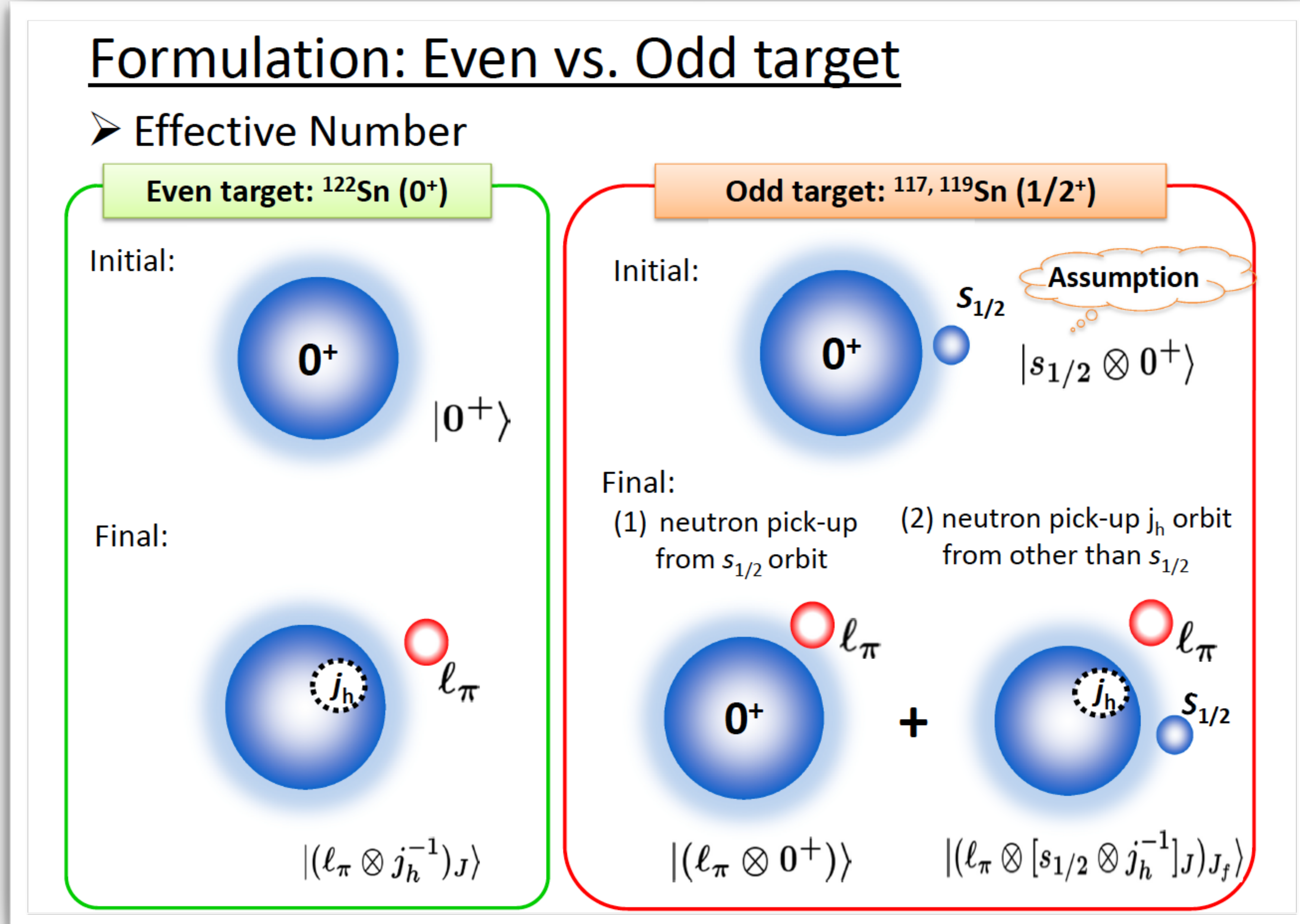

Ikeno@Hadron 2013

Theoretical predictions

Numerical Results: Even vs. Odd target

0 degrees

Even target: ^{122}Sn (0^+) | **Odd target: ^{117}Sn ($1/2^+$)**

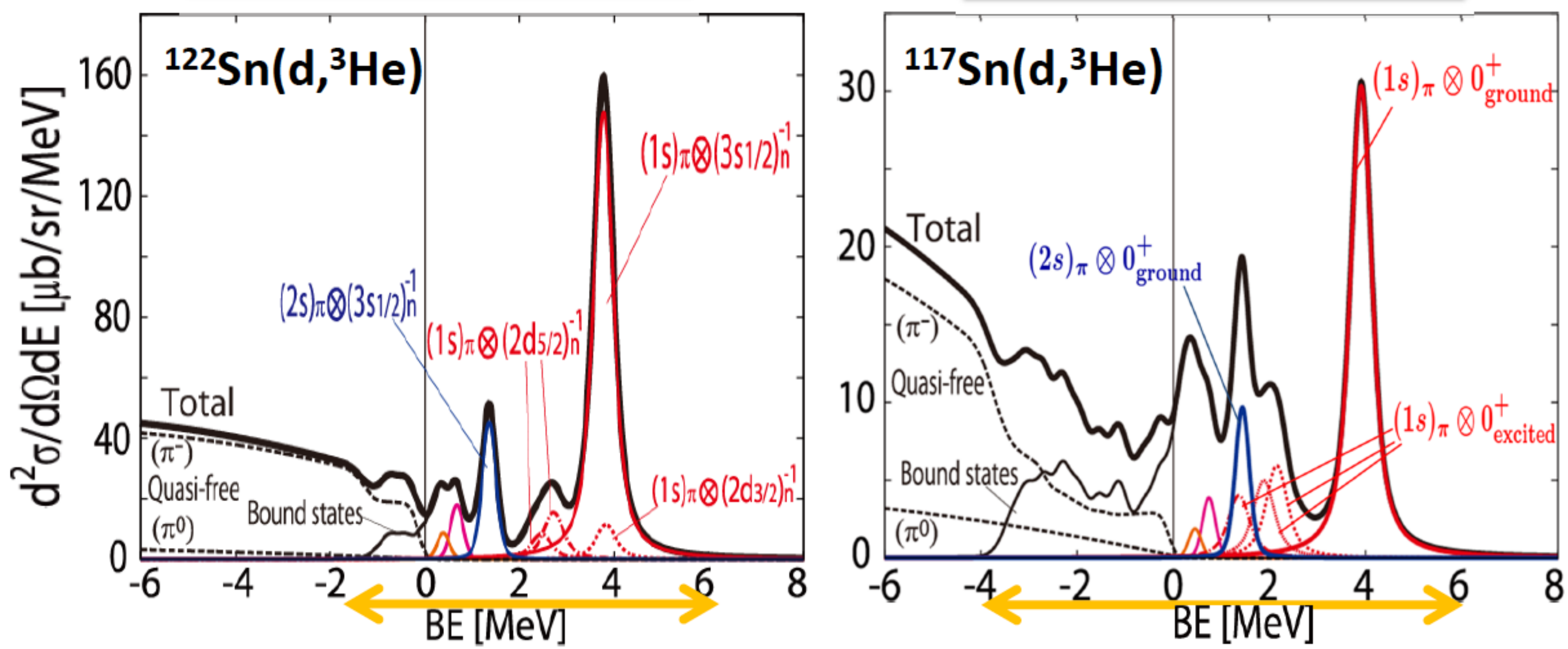

- Pionic 1s state formation with neutron s-hole state is large in both spectra.
- Bound pionic state formation spectra in ^{117}Sn(d,^{3}He) are spread over wider energy range.
- Absolute value of cross section in ^{117}Sn(d,^{3}He) is smaller.

Residual interaction

Formulation: Even vs. Odd target

➢ Effective Number

Even target: ^{122}Sn (0^+)

Initial:

Final:

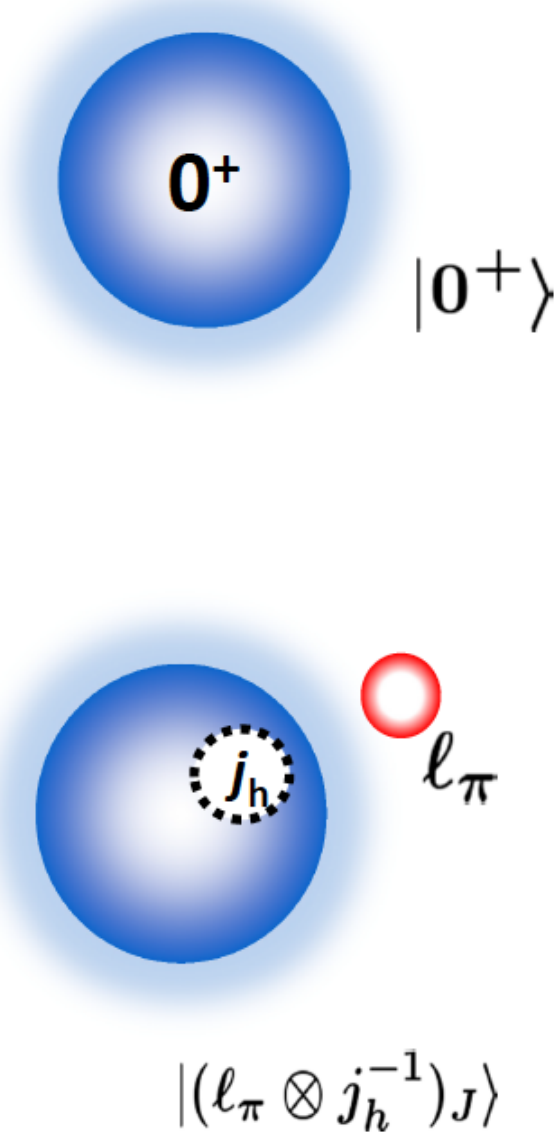

Nose-Togawa et al., PRC71, 061601(R) (2005)

TABLE V. Calculated complex energy shifts because of the residual interaction in ^{131}Sn. The results are shown in units of kilo-electron-volts for $[(1s)_\pi \otimes j_n^{-1}]_J$ and $[(2p)_\pi \otimes j_n^{-1}]_J$, including the s-wave and the p-wave parts of the pion neutron-hole residual interaction.

	$1s$	$2p$	
$s_{1/2}^{-1}$	$-10.5 - 1.3i$	$J = 1/2$	$-3.2 - 0.6i$
		$J = 3/2$	$-3.3 - 0.6i$
		$J = 1/2$	$-7.1 - 2.0i$
$d_{3/2}^{-1}$	$-10.4 - 2.1i$	$J = 3/2$	$0.2 + 0.0i$
		$J = 5/2$	$-3.8 - 1.1i$
		$J = 5/2$	$-3.0 - 1.2i$
$g_{7/2}^{-1}$	$-6.5 - 1.6i$	$J = 7/2$	$0.9 + 0.4i$
		$J = 9/2$	$-2.1 - 0.8i$
		$J = 9/2$	$-4.6 - 1.8i$
$h_{11/2}^{-1}$	$-9.6 - 2.6i$	$J = 11/2$	$1.1 + 0.4i$
		$J = 13/2$	$-3.7 - 1.4i$
		$J = 3/2$	$-5.8 - 1.5i$
$d_{5/2}^{-1}$	$-9.9 - 1.9i$	$J = 5/2$	$0.6 + 0.2i$
		$J = 7/2$	$-3.9 - 1.1i$

Effect of ~10keV

Ikeno@Hadron 2013

$^{122}Sn(d,^{3}He)$ spectra calculated with Neff and Green's function methods

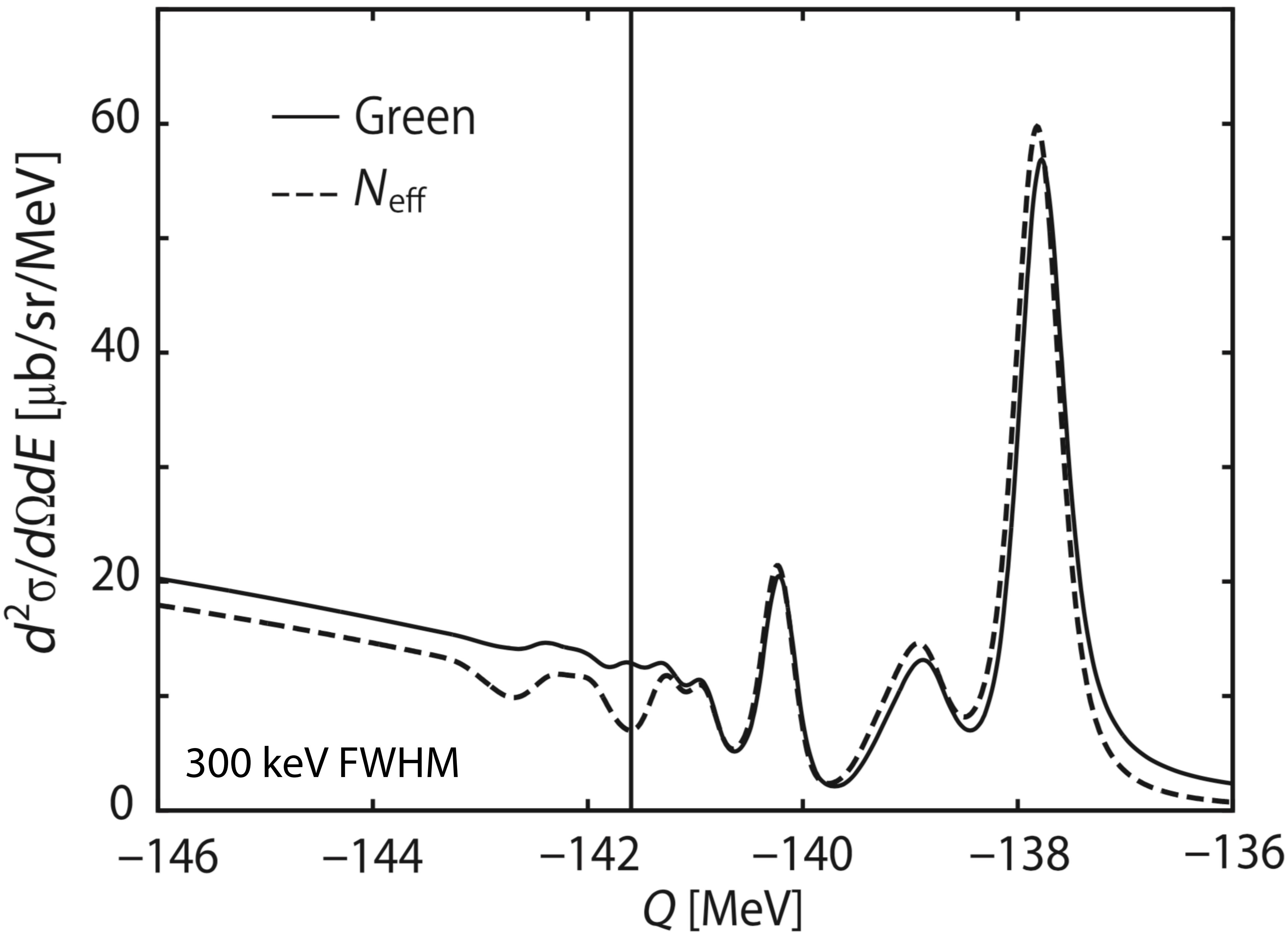

N. Ikeno et al., PTEP 2015, 033D01 (2015)

ρ dependence of chiral condensate

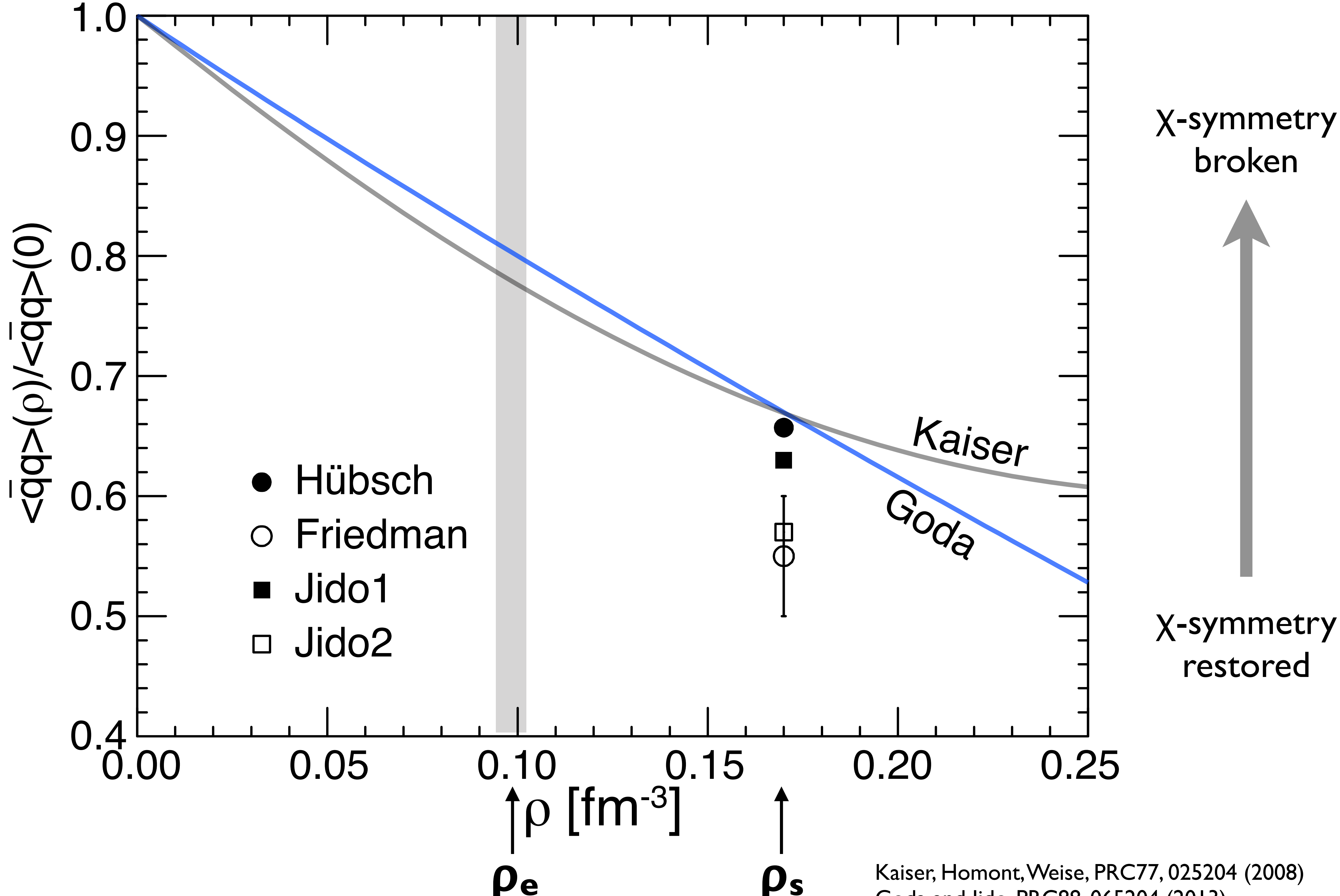

Kaiser, Homont, Weise, PRC77, 025204 (2008)
Goda and Jido, PRC88, 065204 (2013)
Huebsch, Jido, PRC104, 015202 (2021)
Friedman, Gal, PLB792, 340 (2019)
Jido, Hatsuda, Kunihiro, PLB670, 109 (2008)
Lacour, Oller, Meissner, J. Phys. G. 37, 125002 (2010)

Summary

- The binding energies and widths of the 1*s* and 2*p* states in Sn121 were determined with very high precision. Difference between the 1*s* and 2*p* values reduces the systematic errors drastically.
- Recent theoretical progress was adopted for the < qbar q> evaluation, which directly relates the chiral condensate and the pion-nucleus interaction.
- We calculated various corrections for the first time and applied them. The application made a jump of the deduced chiral condensate. After the corrections, the chiral condensate ratio was deduced with much higher reliability.
- We conducted measurement of ρ dependence of chiral condensate in systematic study. We plan measurement with "inverse kinematic" reactions for pionic xenon, which leads to future experiments for pionic unstable nuclei.